Accepted Manuscript

Synthesis of 3-heteryl substituted pyrrolidine-2,5-diones *via* catalytic Michael reaction and evaluation of their inhibitory activity against InhA and *Mycobacterium tuberculosis*

Tetiana Matviiuk, Giorgia Mori, Christian Lherbet, Frédéric Rodriguez, Maria Rosalia Pasca, Marian Gorichko, Brigitte Guidetti, Zoia Voitenko, Michel Baltas

PII: S0223-5234(13)00720-4

DOI: 10.1016/j.ejmech.2013.10.069

Reference: EJMECH 6532

To appear in: *European Journal of Medicinal Chemistry*

Received Date: 25 July 2013

Revised Date: 16 October 2013

Accepted Date: 28 October 2013

Please cite this article as: T. Matviiuk, G. Mori, C. Lherbet, F. Rodriguez, M.R. Pasca, M. Gorichko, B. Guidetti, Z. Voitenko, M. Baltas, Synthesis of 3-heteryl substituted pyrrolidine-2,5-diones *via* catalytic Michael reaction and evaluation of their inhibitory activity against InhA and *Mycobacterium tuberculosis*, *European Journal of Medicinal Chemistry* (2013), doi: 10.1016/j.ejmech.2013.10.069.

Synthesis of 3-heteryl substituted pyrrolidine-2,5-diones *via* catalytic Michael reaction and evaluation of their inhibitory activity against InhA and *Mycobacterium tuberculosis*

Tetiana Matviiuk, Giorgia Mori, Christian Lherbet, Frédéric Rodriguez, Maria Rosalia Pasca, Marian Gorichko, Brigitte Guidetti, Zoia Voitenko, Michel Baltas

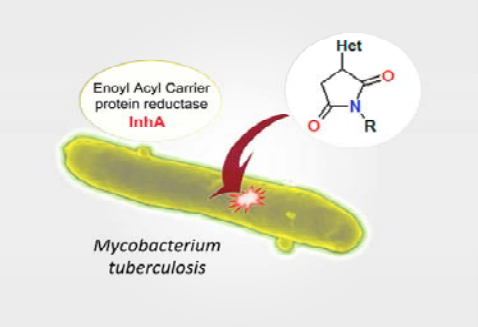

Synthesis of 3-heteryl substituted pyrrolidine-2,5-diones *via* catalytic Michael reaction and evaluation of their inhibitory activity against InhA and *Mycobacterium tuberculosis*

Tetiana Matviiuk,[a,b] Giorgia Mori,[d] Christian Lherbet,*[,a,c] Frédéric Rodriguez,[a,c] Maria Rosalia Pasca,[d] Marian Gorichko,[b] Brigitte Guidetti,[a] Zoia Voitenko,*[,b] Michel Baltas*[,a,c]

[a] *Université de Toulouse; UPS; Laboratoire de Synthèse et Physico-Chimie de Molécules d'Intérêt Biologique, LSPCMIB; 118 route de Narbonne, F-31062 Toulouse cedex 9, France.*

[b] *Taras Shevchenko National University of Kyiv, Department of Chemistry, 64 str. Volodymyrska, Kyiv, 01601, Ukraine. Fax: 38 044 239 3204; Tel: 38 044 239 3315; E-mail: z_voitenko@mail.univ.kiev.ua*

[c] *CNRS; Laboratoire de Synthèse et Physico-Chimie de Molécules d'Intérêt Biologique, LSPCMIB, UMR-5068; 118 Route de Narbonne, F-31062 Toulouse cedex 9, France.*

[d] *University of Pavia; Dipartimento di Biologia e Biotecnologie "Lazzaro Spallanzani", via Ferrata 1, 27100 Pavia, Italy*

Fax: 33 (0)5 61556011; Tel: 33 (0)5 61556289; E-mail:lherbet@chimie.ups-tlse.fr; baltas@chimie.ups-tlse.fr

Keywords : succinimide, Michael addition, tuberculosis, InhA.

Abstract

In the present paper, we report the synthesis *via* catalytic Michael reaction and biological results of a series of 3-heteryl substituted pyrrolidine-2,5-dione derivatives as moderate inhibitors against *M. tuberculosis* H37Rv growth. Some of them present also inhibition activities against InhA.

1. Introduction

Tuberculosis (TB) is the leading cause with malaria and AIDS of worldwide mortality [1]. The effectiveness of current anti-tuberculosis drugs to combat this infection is severely compromised by the emergence of multi- and extensively drug-resistant tuberculosis (MDR-TB [2,3] and XDR-TB [4]). Therefore, new drugs are required to raise the probability to shortly stop all forms of drug-resistant TB. In this context many studies are

based on targeting the cell wall of Mycobacteria and more particularly components essential to its survival. The fatty acid synthase system of *M. tuberculosis* contains unique signature fatty acid, the mycolic acid, which is a central constituent of the mycobacterial cell wall. Mycolic acid biosynthesis is carried out by several successive enzymatic cycles corresponding to two related but distinct Fatty Acid Synthase (FAS) systems, FAS I and II [5]. InhA protein (ENR, EC number: 1.3.1.9) is a key enzyme of FAS II and shows a NADH-dependent enoyl-ACP reductase activity. InhA is a good target as the FAS II system is present in bacteria but is absent in humans. It has already been validated as the primary molecular target of the frontline antitubercular drug isoniazid [6]. Moreover recent studies demonstrated that InhA is also the target for the second line drug ethionamide (ETA) [7].

Michael conjugate addition is a well known effective method in the elaboration of pharmaceutical intermediates, peptide analogues, antibiotics and other drugs [8–10]. In the continuation of our previous study on Michael reaction of heterocyclic substrates with maleimides as electron-deficient dienophiles [11–13], we were interested in expanding not only the boundaries of this reaction but also in applying it for the synthesis of novel pharmaceutical substances. Maleimides are excellent dienophiles/dipolarophiles as well as Michael acceptors. In most cases they usually form succinimide derivatives. This fragment is frequently employed in drug design and defined as promising pharmacophore moiety. Indeed a large number of reported pharmaceutical substances bear a pyrrolidine-2,5-dione core [14,15] including some approved drugs [16] and clinical drug candidates [17].

Pyrrolidine-2,5-dione structural units were also found in numerous natural products. Moiramide B and Andrimide (Fig. 1) have been described as new highly specific antibiotics [18] exhibiting potent antibacterial activity against methicillin-resistant

Staphylococcus aureus and a range of other antibiotic-resistant human pathogens. These natural products were identified to target FAS system that is also the primary target for antitubercular drugs [19]. Furthermore, Hirsutellones A–E (Fig. 1), a family of novel alkaloids, were reported to display significant growth inhibitory activity against *Mycobacterium tuberculosis* H37Rv strain [20].

Herein we report complementary results on synthesis of selected 3-heteryl substituted succinimide derivatives *via* catalytic conjugated addition of nucleophilic heterocycles to maleimides. We also report our first findings showing the encouraging activities against *M. Tuberculosis* H37Rv growth and/or inhibitory ones against InhA of some of the compounds synthesized.

2. Results and discussion

2.1. Chemistry

N-Aryl maleimides were used as electron-deficient substrates in conjugate addition with nucleophilic heterocycles.

The first heterocycle in our investigation was 4*H*-1,2,4-triazole-3-thiole (**1**) (Scheme 1). This substrate was selected because a large number of reported molecules bearing this structural unit possess antibacterial, [21], antimicrobial [22] and antitubercular properties [23]. In the Michael addition with maleimides, as we have very recently reported [24], the ambident nucleophile **1** gives the conjugated products *via* a more nucleophilic exocyclic mercapto group as a single type of products (Scheme 1). The highest yields of the adducts **2a,b** were obtained in the presence of catalytic amount of $AlCl_3$ (1.5%) (Table 1). Lithium perchlorate has shown lower catalytic efficacy than aluminium chloride for the formation of products **2a,b**.

Scaffold **3** was then selected for the synthesis of pyrrolidine-2,5-dione derivatives **4a,b**. These compounds were designed as analogues of known nanomolar inhibitor of InhA protein GEQ (Fig. 2) [25]. The 1-(9*H*-fluoren-9-yl)-piperazine group of this inhibitor has been shown to be an important pharmacophore and is responsible for extensive hydrophobic interactions in the binding site of InhA protein [26]. Compounds **4a** and **4b** were synthesized *via* C–N Michael addition of 1-(9*H*-fluoren-9-yl)piperazine (**3**) to *N*-phenyl and *N*-benzyl maleimides (Scheme 2). The best results were obtained when catalytic amount of lithium perchlorate was used (Table 1). Aluminium chloride appears to be not an effective catalyst in this case.

Thereafter, Michael addition of *N*-aryl substituted maleimides was carried out with 1,2,3,4-tetrahydroisoquinoline (THIQ) (**5**) (Scheme 2). Simple THIQs were found in several plants and mammalian species. Moreover, THIQs are the constituents of several drugs and they exhibit antibacterial, [27] antitubercular [28] and antimicrobial [29] activities. As for compound 3, reaction with 1,2,3,4-tetrahydroisoquinoline (THIQ) afforded the best yields of the products **6a,b** when lithium perchlorate ($LiClO_4$) was added as catalyst to the reaction mixture in dry dioxane at room temperature (method A). Another synthetic approach using Hünig's base (Method B) was applied for the synthesis of the adducts 4a,b and 6a,b but the yields were lower than in the case of $LiClO_4$ catalysis (Table 1).

1*H*-Imidazole (**7**), a substrate with well-known range of bioactivity, was selected for further C–N addition studies. The reaction proceeds in excellent yield as was recently reported by us [24].

Finally, Michael addition was carried out between *N*-substituted maleimides and two

bulky C-H active heterocycles – 2-phenylindolizine (**9**) and 7,9-dinitropyrido[2,1-a]isoindole (**10**) (Scheme 3). Lithium perchlorate appears to be not effective as catalyst in the case of C–C bond formation; only traces of the desired products were isolated. Different other Lewis acids have been then tested without success ($ZnCl_2$, $SnCl_4$, $TiCl_4$, $BiCl_3$). The products corresponding to C–C conjugated addition **11a**,**b** and **12** were obtained in good yields only when anhydrous aluminium chloride was used as catalyst (Scheme 3, Table 1). The structure of these 3-substituted indolizine compounds was confirmed by NOESY experiments (See supporting information). A correlation could be found between the alpha hydrogen atom of the succinimide and the H-5 of indolizine.

Thereby, in the course of this study, we have found that lithium perchlorate is an efficient catalyst for C–N conjugate addition when aluminium chloride demonstrates high efficacy for C–C addition reaction.

2.2. Biology

2.2.1. Antimycobacterial activities

All synthesized compounds were evaluated by determining the minimal inhibitory concentration (MIC) on *M. tuberculosis* H37Rv strain [30,31]. They were also evaluated *in vitro* as potential InhA inhibitors at 50 µM by applying a commonly used method [32] Recombinant *M. tuberculosis* InhA was expressed in *E. coli* and subsequently purified according to a previous reported procedure [32]. The results are shown in Table 2. Well known InhA inhibitors Triclosan [33], GEQ [25] and Isoniazid as H37Rv strain inhibitors were used for comparison. The latter (Genz-10855) has been reported to display significantly high binding affinity and selectivity to the InhA protein but in the same time poor growth inhibitory activity on *Mycobacterium tuberculosis*.

Compounds **4a** and **4b** present the best activities on InhA protein among the tested derivatives. Nevertheless the values are still too modest compared to that of GEQ. In the same time, unlike GEQ, MIC values of compounds **4a** and **4b** are much better (Table 2).

Molecular docking evaluation was performed to understand the differences in binding of reported nanomolar inhibitor and our analogues with pyrrolidine-2,5-dione substituent. Two enantiomers (*R* and *S*) of the compound **4a** and GEQ were docked into the binding site of InhA by applying the same calculation algorithm and procedure. The best binding modes of investigated molecules are represented in Fig. 2. Docking was carried out taking into account flexibility of 11 amino acid residues from the lateral chains (including Tyr158) and cofactor NAD^+ as a set of features in the binding pocket of the protein. The RMSD value between crystallographic conformation (PDB entry 1P44, chain A) [26] and the best docking mode of GEQ (with the best scoring data) is 0.6 Å, that could be a proof of the prediction ability of applying screening procedure.

Some predicted differences in the mode of binding of **4a** (*R* and *S*) are observed (Fig. 2) compared to GEQ. From the alignment of binding complexes (obtained from the docking studies and crystallographic data for InhA complex with GEQ inhibitor), we could summarize that **4a** could be inserted in the active site but through a different geometry depending on the enantiomer used. Indeed, the fluorenyl ring could not exactly match the large hydrophobic pocket of InhA protein. It is also worth mentioned that electrostatic interactions and hydrogen bonding between **4a** and cofactor NAD^+ are missing (at least for one enantiomer), relative to the corresponding crystallographic inhibitor GEQ (see supporting information: 2D ligand-protein interaction map). Neverless, docking results for both enantiomers are similar (See supporting information) and show lower score values by comparison with GEQ. These results are in accordance with the biological results.

Compound **12** shows an inhibitory activity similar to compounds **4a** and **4b**. It is noteworthy that both compounds **12** and **4** contain rigid tricyclic structural fragments, while compounds **6a**,**b** and **8a**,**b** have more flexible and non-planar moieties.

Interestingly, compound **6a** presents high inhibition activity on bacteria growth while derivative **6b** shows a reduced one. These inhibitor structures are interesting for further investigation. Due to their low inhibition of InhA, compounds **6a** and **6b** might present a different mechanism of action and target other proteins involved in bacteria growth. Synthesized derivatives of 4*H*-1,2,4-triazole-3-thiole **2a** and **2b** have shown also good inhibition values on bacteria but as for compounds **6a**, **6b** they have presented poor activity on the protein.

Finally, the MIC evaluations of synthesized compounds have shown that in their majority, they displayed higher activities than GEQ (Table 2). The best results were obtained for isoquinoline (**6a**, **6b**) and 4*H*-1,2,4-triazole-3-thiol (**2a** and **2b**) derivatives. These two groups of structurally different functionalized succinimides might constitute an attractive starting point for further development of antituberculosis agents. It is also noteworthy that GEQ analogues **4a,b** show much higher inhibition of *M. tuberculosis* than GEQ itself. Finally, moderate values of MIC were determined for the derivatives of 2-phenylindolizine **11a,b**, 7,9-dinitropyrido[2,1-a]isoindole **12** and imidazole **8a,b**.

2.2.2. Cytotoxicities of the compounds

The cytotoxicity of different 3-heteryl substituted pyrrolidine-2,5-dione derivatives was evaluated on two human cell lines, the human colon cancer cell line HCT116 and the human fibroblast cell line GM637 (Table 2). The data showed that the IC_{50} of the different compounds tested were above 100 μM, indicating that these compounds are not cytotoxic against human cell lines. Only one exception was found for compound **2a** bearing a 4*H*-1,2,4-triazole-3-thiole moiety. The results show that this compound is clearly cytotoxic against human cell lines in the micromolar range.

3. Conclusion

A series of 3-heteryl substituted pyrrolidine-2,5-dione derivatives were prepared and assayed for the inhibition of InhA and *M. tuberculosis* growth. Lewis acids were found to be effective and easy handling catalysts in Michael conjugated addition of nucleophilic heterocycles to *N*-aryl substituted maleimides. Among the synthesized molecules, compounds **4a**, **4b** and **12** displayed moderate inhibition activities against InhA that are the best among compounds evaluated and poor activities on *M. tuberculosis.* More interesting, compounds **2a**, **2b**, **6a** and **6b** derived from 4*H*-1,2,4-triazole-3-thiol and 1,2,3,4-tetrahydroisoquinoline respectively, exhibit good inhibition values on bacterial growth. It is important to know that, while compound **2a** is cytotoxic, molecules **6a** and **6b** are not, so that they can be subjected for optimization in order to gain access to new leads of antitubercular agents. Furthermore, replacing one of the structural parts of GEQ for a pyrrolidine-2,5-dione ring led to increased activities against *M. tuberculosis* H37Rv.

4. Experimental Section

4.1. Material

All chemicals were obtained from Aldrich or Acros Organics and used without further purification. All solvents were distilled before use. Compounds **3**, **9** and **10** have been synthesized according to the literature procedures [34, 35, 36 respectively] and completely characterized using ^{1}H and ^{13}C NMR and MS. Nuclear magnetic resonance spectra were recorded on a 'Mercury 400' Varian spectrometer (^{1}H, ^{13}C NMR; TMS signal was used as an internal standard for calibration of spectral data) and on a Bruker AC 300 spectrometer (^{1}H, ^{13}C NMR; solvent residue signals were used for calibration of spectral data). Mass spectrometry (MS) data were obtained on a ThermoQuest TSQ 7000 spectrometer, high-resolution mass spectra (HRMS) were recorded on a ThermoFinnigan MAT 95 XL

spectrometer using chemical ionization (CI; CH_4 or NH_3) and electrospray ionization (ESI) methods. Melting points were measured on a Mettler Toledo MP50 melting point system.

4.2. Chemistry

4.2.1. General procedure for C-S Michael addition (Compounds **2a,b**): compounds **2a** and **2b** were synthesized as previously reported [24].

4.2.1.1. 1-Phenyl-3-(4H-1,2,4-triazol-3-ylsulfanyl)-2,5-pyrrolidinedione (2a).

Yield 62 %; mp: 154-155 °C. ^{1}H NMR (400 MHz, DMSO-d_6): δ = 2.92 (dd, J = 18.0 Hz, J = 4.8 Hz, 1H), 3.42 (dd, J = 18.0 Hz, J = 9.6 Hz, 1H), 4.67 (dd, J = 4.8 Hz, J = 9.6 Hz, 1H), 7.26 (d, J = 7.2 Hz, 2H), 7.40–7.53 (m, 3H), 8.56 (s, 1H), 14.08 (br s, 1H). ^{13}C NMR (100 MHz, DMSO-d_6): δ = 36.5, 41.3, 127.0, 128.5, 128.9, 132.8, 145.8, 155.4, 174.3, 174.8. HRMS calculated for $C_{12}H_{11}N_4O_2S$ 275.0603; found 275.0596.

4.2.1.2. 1-(4-Methoxyphenyl)-3-(4H-1,2,4-triazol-3-ylsulfanyl)-2,5-pyrrolidinedione (2b).

Yield 63 %; mp: 162-163 °C. ^{1}H NMR (400 MHz, DMSO-d_6): δ = 2.93 (dd, J = 16.8 Hz, J = 2.4 Hz, 1H), 3.40 (dd, J = 16.8 Hz, J = 9.4 Hz, 1H), 3.82 (s, 3H), 4.54 (dd, J = 2.4 Hz, J = 9.4 Hz, 1H), 6.98 (d, J = 8.2 Hz, 2H), 7.19 (d, J = 8.2 Hz, 2H), 8.04 (s, 1H), 14.17 (br s, 1H). ^{13}C NMR (100 MHz, DMSO-d_6): δ = 36.3, 41.0, 54.8, 128.1, 128.9, 129.4, 132.8, 140.5, 145.7, 155.4, 158.8, 172.9, 173.5. MS [M+H$^+$] calculated for $C_{13}H_{13}N_4O_3S$ 305.3; found 305.3. HRMS: calculated for $C_{13}H_{13}N_4O_3S$ 305.0708; found 305.0707.

4.2.2. General procedure for C–N Michael addition: compounds **8a** and **8b** were synthesized as previously reported [24].

Method A (*compounds* **4a,b**, **6a,b**, **8a,b**): To a solution of 1-(9*H*-fluoren-9-yl)piperazine **3**, 1,2,3,4-tetrahydroisoquinoline **5** or 1*H*-imidazole **7** (0.19 mmol) in dry dioxane *N*-substituted maleimide (0.22 mmol) was added. The mixture was stirred for 15 minutes to dissolve the reagents, then catalytic amount of $LiClO_4{\cdot}3H_2O$ (4 mg, 0.02 mmol) was added. The reaction

mixture was stirred overnight at room temperature. The reaction progress was controlled by TLC. After completion, the solvent was evaporated and the crude product was purified by flash chromatography.

Method B (*compounds* **4a,b**, **6a,b**): To a solution of amine (0.28 mmol) in *i*PrOH, *N*-phenyl maleimide (0.34 mmol) was added. After 10 min stirring, *N,N'*-diisopropylethylamine was added (0.15 mmol). The reaction mixture was stirred overnight at room temperature. Then the solvent was evaporated under reduced pressure and the corresponding crude product was purified by flash chromatography.

4.2.2.1. 3-[4-(9H-Fluoren-9-yl)-1-piperazinyl]-1-phenyl-2,5-pyrrolidinedione (4a).

The crude product was purified by flash chromatography (silica, CH_2Cl_2:EtOAc = 8:2) to give light yellow crystals. Yield: 88% (method A), 70% (method B); mp: 191-192 °C. ^{1}H NMR (300 MHz, $CDCl_3$): δ = 2.61–3.04 (m, 10H), 3.92 (dd, J = 4.8 Hz, J = 9.0 Hz, 1H), 4.85 (s, 1H), 7.24–7.49 (m, 9H), 7.63–7.10 (m, 4H). ^{13}C NMR (75 MHz, $CDCl_3$): δ = 32.1, 48.9, 49.9, 62.6, 69.9, 119.8, 126.1, 126.5, 127.1, 128.3, 128.8, 129.2, 131.6, 141.1, 143.7, 174.2, 175.1. HRMS: calculated for $C_{27}H_{26}N_3O_2$ 424.2020; found 424.2017.

4.2.2.2. 1-Benzyl-3-[4-(9H-fluoren-9-yl)-1-piperazinyl]-2,5-pyrrolidinedione (4b).

Yield: 83% (method A), 58% (method B); mp: 168-169 °C. ^{1}H NMR (300 MHz, DMSO-d_6): δ = 2.52–2.99 (m, 10H), 3.81 (dd, J = 4.5 Hz, J = 9.0 Hz, 1H), 4.53 (s, 2H) 4.77 (s, 1H), 7.25–7.67 (m, 13H). ^{13}C NMR (75 MHz, $CDCl_3$): δ = 31.7, 48.8, 49.8, 50.5, 62.4, 69.8, 120.0, 126.1, 126.7, 127.0, 128.2, 128.9, 129.3, 131.5, 140.9, 143.2, 174.6, 179.8. HRMS: calculated for $C_{28}H_{28}N_3O_2$ 438.2176; found 438.2180.

4.2.2.3. 3-(3,4-Dihydroisoquinolin-2(1H)-yl)-1-phenylpyrrolidine-2,5-dione (6a).

The crude product was purified by flash chromatography (silica, PE:EtOAc = 7:3) to give a white powder. Yield: 87%; mp: 149-150 °C. ^{1}H NMR (300 MHz, DMSO-d_6): δ = 2.79–3.10 (m, 6H), 3.72 (d, J = 14.7 Hz, 1H), 4.09 (d, J = 14.7 Hz, 1H), 4.27 (dd, J = 5.7 Hz, J = 8.7 Hz,

1H), 7.06–7.12 (m, 4H), 7.29–7.32 (m, 2H), 7.40–7.53 (m, 3H). ^{13}C NMR (75 MHz, DMSO-d_6): δ = 29.0, 31.4, 46.5, 50.9, 62.2, 125.5, 126.0, 126.4, 127.2, 128.4, 128.6, 128.9, 132.3, 133.9, 134.5, 174.6, 175.7. HRMS calculated for $C_{19}H_{19}N_2O_2$ 307.1447; found 307.1453.

4.2.2.4. 1-Benzyl-3-(3,4-dihydroisoquinolin-2(1H)-yl)pyrrolidine-2,5-dione (6b).

The crude product was purified by flash chromatography (silica, PE:EtOAc = 3:2) to give creamy crystals. Yield: 79%; mp: 106-107 °C. ^{1}H NMR (300 MHz, DMSO-d_6): δ = 2.64–2.99 (m, 6H), 3.57 (d, J = 14.7 Hz, 1H), 3.98 (d, J = 14.7 Hz, 1H), 4.18 (dd, J = 5.4Hz, J = 8.4 Hz, 1H), 4.59 (s, 2H), 6.97–7.12 (m, 4H), 7.25–7.37 (m, 5H). ^{13}C NMR (75 MHz, DMSO-d_6): δ = 29.0, 31.1, 41.2, 46.4, 50.8, 61.9, 125.5, 126.0, 126.3, 127.4, 127.5, 128.4, 128.5, 133.8, 134.3, 136.2, 175.3, 176.5. HRMS calculated for $C_{20}H_{21}N_2O_2$ 321.1603; found 321.1610.

4.2.2.5. 3-(1H-Imidazol-1-yl)-1-phenyl-2,5-pyrrolidinedione (8a).

Yield 95 %; mp: 161-163 °C. ^{1}H NMR (400 MHz, DMSO-d_6): δ = 3.16 (dd, J = 16.8 Hz, J = 6.4 Hz, 1H), 3.40 (dd, J = 16.8 Hz, J = 9.2 Hz, 1H), 5.68 (dd, J = 9.2 Hz, J = 6.4 Hz, 1H), 6.92 (s, 1H), 7.36–7.49 (m, 5H), 7.57 (s, 1H), 7.80 (s, 1H). ^{13}C NMR (100 MHz, DMSO-d_6): δ = 36.9, 54.8, 118.6, 127.3, 128.6, 128.9, 129.3, 132.5, 138.0, 172.9, 173.4. HRMS: calculated for $C_{13}H_{12}N_3O_2$ 242.0924; found 242.0918.

4.2.2.6. 3-(1H-Imidazol-1-yl)-1-(4-methoxyphenyl)-2,5-pyrrolidinedione (8b).

Yield 92 %; mp: 154-155 °C. ^{1}H NMR (400 MHz, DMSO-d_6): δ = 3.18 (dd, J = 16.8 Hz, J = 6.8 Hz, 1H), 3.37 (dd, J =16.8 Hz, J = 4.2 Hz, 1H), 3.83 (s, 3H), 5.64 (dd, J = 4.2 Hz, J = 6.8 Hz, 1H), 6.94 (s, 1H), 7.00–7.26 (m, 4H), 7.40 (s, 1H), 7.83 (s, 1H). ^{13}C NMR (100 MHz, DMSO-d_6): δ = 37.9, 53.8, 55.2, 114.9, 120.0, 127.5, 127.6, 132.8, 137.9, 159.9, 170.1, 172.7. HRMS: calculated for $C_{14}H_{14}N_3O_3$ 272.1030; found 272.1035.

4.2.3. General procedure for C–C Michael addition, (compounds **11a** and **11b** *)*: Compounds **11a**, **11b** were synthesized as previously reported [24].

4.2.3.1. 1-Phenyl-3-(2-phenyl-3-indolizinyl)-2,5-pyrrolidinedione (11a).

The crude product was purified by flash chromatography (EtOAc : PE / 2 : 8) to afford the desired compound as light green crystals. Yield: 84%; mp: 210-211 °C. ^{1}H NMR (300 MHz, DMSO-d_6): δ = 3.06 (dd, J = 6.9 Hz, J = 17.7 Hz, 1H), 3.32–3.37 (m, 1H), 5.13 (t, J = 8.4 Hz, 1H), 6.60–7.54 (m, 14H), 7.97 (d, J = 6.6 Hz, 1H). ^{13}C NMR (75 MHz, DMSO-d_6): δ = 33.6, 37.4, 99.6, 111.3, 114.5, 117.5, 119.1, 122.8, 126.9, 127.1, 128.4, 128.7, 128.9, 129.0, 129.8, 132.3, 132.5, 135.7, 174.5, 175.8. HRMS: calculated for $C_{24}H_{19}N_2O_2$ 367.1441; found 367.1436.

4.2.3.2. 1-Benzyl-3-(2-phenyl-3-indolizinyl)-2,5-pyrrolidinedione (11b).

The crude product was purified by flash chromatography (EtOAc : PE / 2 : 8) to afford the desired compound as light grey powder. Yield: 71%; mp: 192–194 °C. ^{1}H NMR (300 MHz, DMSO-d_6): δ = 3.14 (dd, J = 6.3 Hz, J = 16.8 Hz, 1H), 3.33–3.37 (m, 1H), 4.51 (s, 2H) 5.07 (t, J = 9.0 Hz, 1H), 6.67–7.53 (m, 14H), 7.95 (d, J = 6.9 Hz, 1H). ^{13}C NMR (75 MHz, DMSO-d_6): δ = 33.6, 37.5, 46.6, 99.8, 111.5, 114.3, 117.1, 118.9, 123.0, 126.4, 127.1, 128.4, 128.7, 129.1, 129.3, 129.8, 132.3, 132.4, 135.7, 173.8, 176.1. HRMS: calculated for $C_{25}H_{21}N_2O_2$ 381.1598; found 381.1605.

4.2.3.3. 3-(7,9-Dinitropyrido[2,1-a]isoindol-6-yl)-1-phenyl-2,5-pyrrolidinedione (12).

7,9-Dinitropyrido[2,1-*a*]isoindole **10** (100 mg, 0.39 mmol) was dispersed in dry dioxane. Then *N*-substituted maleimide (0.4 mmol) was added. The mixture was stirred for 15 minutes. Thereafter anhydrous aluminium chloride (3 mg, 0.022 mmol) was quickly added. The reaction mixture was refluxed over 6 h. The progress of the reaction was monitored by TLC. After reaction completion, the solvent was evaporated under reduced pressure and the crude

product was recrystallized from DMSO to afford a red powder. Yield: 62%; mp: 290−292 °C. ^{1}H NMR (300 MHz, DMSO-d_6): δ = 3.27 (dd, J = 8.2 Hz, J = 18.3 Hz, 1H), 3.79 (dd, J = 9.8 Hz, J = 18.3 Hz, 1H), 5.47 (t, J = 9.0 Hz, 1H), 7.35–7.78 (m, 7H), 8.88 (d, J = 2.1 Hz, 1H), 8.99–9.06 (m, 2H), 9.88 (d, J = 2.1 Hz, 1H). ^{13}C NMR (75 MHz, DMSO-d_6): δ = 34.7, 47.8, 110.8, 111.2, 121.4, 127.3, 128.5, 128.9, 131.4, 132.1, 132.6, 135.2, 136.1, 139.0, 147.0, 148.9, 150.5, 175.4, 179.2. HRMS: calculated for $C_{22}H_{15}N_4O_6$ 431.0986; found 431.0992.

4.3. Biology

4.3.1. Growth conditions and minimum inhibitory concentration (MIC) determination. M. tuberculosis H37Rv was used as the reference strain. The strains were grown at 37 °C in Middlebrook 7H9 broth (Difco), supplemented with 0.05% Tween 80, or on solid Middlebrook 7H11 medium (Difco) supplemented with oleic acid-albumin-dextrose-catalase (OADC). MICs for the new compounds were determined by means of the micro-broth dilution method. Dilutions of *M. tuberculosis* wild-type cultures (about 10^5–10^6 cfu/ml) were streaked onto 7H11 solid medium containing a range of drug concentrations (0.25 μg/mL to 40 μg/mL). Plates were incubated at 37 °C for about 21 days and the growth was visually evaluated. The lowest drug dilution at which visible growth failed to occur was taken as the MIC value. Results were expressed as the average of at least three independent determinations.

4.3.2. Cytotoxicity of the compounds

Human colon cancer cell line HCT116 (ATCC) and human fibroblasts (GM637 cell line) were cultured in DMEM supplemented with 10% fetal calf serum. For cytotoxicity evaluation, 3000 cells were seeded per well in 96-wells plates and, 24 h later, were treated with 9 concentrations ranging from 100 nM to 100 μM (8 replicates for each). After 4 days of

treatment, the cytotoxicity of each compound was measured by using the WST-1 kit (Roche). IC_{50} values were determined by using PRISM software (GraphPad).

4.3.3. InhA expression and purification.

Recombinant *M. tuberculosis* InhA was expressed in *E. coli* and subsequently purified. The production and purification of the protein were performed as described in the reference [32].

4.3.4. Inhibition Kinetics

Stock solutions of all compounds were prepared in DMSO such that the final concentration of this co-solvent was constant at 5% v/v in a final volume 1 mL for all kinetic reactions. Kinetic assays using *trans*-2-dodecenoyl-Coenzyme A (DD-CoA) and wild-type InhA were performed as described [32]. Reactions were initiated by addition of InhA (100 nM final) to solutions containing DD-CoA (50 μM final), inhibitor, and NADH (250 μM final) in 30 mM PIPES, 150 mM NaCl, pH 6.8, buffer. Control reactions were carried out with the same conditions as described above but without inhibitor. The inhibitory activity of each derivative was expressed as the percentage inhibition of InhA activity with respect to the control reaction without inhibitor. All activity assays were performed in triplicate.

4.4. Molecular docking studies

Molecular docking studies were performed using Molegro Virtual Docker 5.5 software (CLC Bio, Aarhus, Denmark). Molecular graphics and some analyses were performed with the UCSF Chimera package. Chimera is developed by the Resource for Biocomputing, Visualization, and Informatics at the University of California, San

Francisco (supported by NIGMS P41-GM103311). The Protein structures optimization and preparation (structure checks, rotamers, protonation analysis) were done using Accelrys Discovery Studio 3.0 client and UCSF Chimera 1.6.2 or 1.7 (Dock Prep without minimization). The Ligand structures were extracted (SciTE text editor) from aligned protein structure or sketched using ChemAxon Marvin 5.5 and prepared for the docking studies (3D structure optimization, hybridization checking, protonation) using Discovery Studio 3.0 client. After analyzing of known crystallographic structures of InhA, 1P44 pdb entry (chain A, X-ray, 2.7 Å resolution) [26] from Protein Data Bank [37] includes NAD^+/NADH and ligand structure (GEQ) in the active site was chosen as protein molecular structure for further docking studies. The cavity detection algorithm implemented in MVD was used to optimize the definition of a 15 Å (radius) potential binding site but not for constraining results to the cavity. The corresponding crystallographic NAD^+ structure was taken into account as cofactor using the MVD feature possibilities. No water molecules were included into the docking procedure. The side chains around compound **4a** (11 residues) were set flexible during the calculation. Combination of different calculation (Moldock SE, Moldock Optimizer) algorithms and scoring schemes (Moldock, Plants) were tested [38,39] giving insight similar top binding modes for GEQ and compound **4a**. After calculation, minimization steps (global, lateral chain, ligands) and optimization of hydrogen bonds were done using MVD default features followed by clustering. Using these conditions the crystallographic conformation of GEQ was reproduced with a good accuracy (less than 0.6 Å of RMSD with reference structure 1P44a) and nearly no fluctuation of flexible residues including Tyr158 was recorded. Subsequently optimized parameters were applied to the docking procedure. The enantiomers *R* and *S* of compound **4a** were screened to understand differences in binding of our compounds compared to the reference ligand. The results are represented on **Fig. 2**.

The graph representation of normalized descriptors LE1 (Molegro's Moldock Score divided by heavy atoms number) *vs* LE3 (Molegro's Rerank score divided by heavy atoms number) obtained from the docking studies of compound **4a** (*R*- and *S*-enantiomers) and GEQ (60 calculation runs followed by clustering of results) is shown on **SI Fig. 1** (See supporting information). Evidently, the best binding poses (circles colored in red) with the lowest energy correspond to GEQ structure (the worst values correspond to poses outside the binding site) that are in correlation with obtained biological results.

Acknowledgments

T. Matviiuk was supported by French Embassy in Kiev, Ukraine. The investigations having been performed within the framework of the GDRI (Groupement Franco-Ukrainien en Chimie Moléculaire; between UPS, Toulouse and Taras Shevchenko National University of Kiev).

References

[1] World Health Organization: http://www.who.int/tb/publications/global_report/2010/en/index.html

[2] M.H. Cynamon, Y. Zhang, T. Harpster, S. Cheng, M.S. DeStefano, High-dose isoniazid therapy for isoniazid-resistant murine Mycobacterium tuberculosis infection, Antimicrob. Agents Chemother. 43 (1999) 2922-2924.

[3] P. Bemer-Melchior, A. Bryskier, H.B. Drugeon, Comparison of the in vitro activities of rifapentine and rifampicin against Mycobacterium tuberculosis complex, J. Antimicrob. Chemother. 46 (2000) 571-576.

[4] A. Jain, R. Mondal, Extensively drug-resistant tuberculosis: current challenges and threats, FEMS Immunol. Med. Microbiol. 53 (2008) 145-150.

[5] (a) H. Marrakchi, F. Bardou, M.-A. Laneelle, M. Daffe, «*The Mycobacterial Cell Envelope*», D. Mamadou and J. M. Reyrat, eds., 2008, 41, ASM Press, Washington DC. (b) K. Bloch, Control mechanisms for fatty acid synthesis in Mycobacterium smegmatis, Adv. Enzymol. Relat. Areas Mol. Biol. 45 (1977) 1-84.

[6] A. Banerjee, E. Dubnau, A. Quemard, V. Balasubramanian, K.S. Um, T. Wilson, D. Collins, G. de Lisle, W.R. Jacobs, InhA, a gene encoding a target for isoniazid and ethionamide in Mycobacterium tuberculosis, Science 263 (1994) 227-230.

[7] F. Wang, R. Langley, G. Gulten, L. G. Dover, G.S. Besra, W.R. Jacobs Jr., J. C. Sacchettini, Mechanism of thioamide drug action against tuberculosis and leprosy. J. Exp. Med. 204 (2007) 73-78.

[8] R. Y. Shrestha, K. A. Shen, J-S. A. Pollack, J.S. Taylor, K.L. Wooley, Dual peptide nucleic acid- and peptide-functionalized shell cross-linked nanoparticles designed to target mRNA toward the diagnosis and treatment of acute lung injury, Bioconjug. Chem. 33 (2012) 574-585.

[9] S. Harada, N. Kumagai, T. Kinoshita, S. Matsunaga, M. Shibasaki, Direct catalytic asymmetric Michael reaction of hydroxyketones: asymmetric Zn catalysis with a Et2Zn/linked-BINOL complex, J. Am. Chem. Soc. 125 (2003) 2582-2590.

[10] G. Bartoli, M. Bosco, A. Carlone, A. Cavalli, M. Locatelli, A. Mazzanti, P. Ricci, L. Sambri, P. Melchiorre, Organocatalytic asymmetric conjugate addition of 1,3-dicarbonyl compounds to maleimides, Angew. Chem. Int. Ed. 45 (2006) 4966-4970.

[11] Z.V. Voitenko, O.A. Pokholenko, O.O. Shkarov, O.V. Shishkin, S.V. Shishkina, A. Dall'ava, M. Vedrenne, M. Sanchez, Structure of the Cycloaddition Products of Pyrido[2,1-*a*]isoindole with Maleimide Derivatives: X-ray Diffraction Analysis and ^{1}H NMR Variable-Temperature Spectra, Eur. J. Org. Chem. 7 (2001) 1401-1405.

[12] Z.V. Voitenko, O.A. Pokholenko, O.O. Shkarov, V.O. Kovtunenko, F.S. Babichev, Cycloaddition in Condensed Isoindoles. 2. Method for Obtaining New Derivatives of 2-Phenylpyridine, Chem. Heterocycl. Compd. 38 (2002) 190-196.

[13] T. Matviiuk, M. Gorichko, A. Kysil, S. Shishkina, O. Shishkin, Z. Voitenko, Catalysis by Lithium Perchlorate Enables Double-Conjugate Addition of Electron-Deficient Maleimides to 2-Aminopyridines and 2-Aminothiazoles, Synth. Comm. 42 (2012) 3304-3310.

[14] (a) A. Mitchinson, A. Nadin, Saturated nitrogen heterocycles, J. Chem. Soc. Perkin Trans. 1 (2000) 2862-2892. (b) M. Pinchon, B. Figadere, Synthesis of 2,5-disubstituted pyrrolidines, Tetrahedron: Asymmetry 7 (1996) 927-964.

[15] A.M. Criderl, P.H. Andersenz, S.F. Cruel, D. Ghoshl, A. Harpalani, 3-Phenylpyrrolidines: synthesis and evaluation of the *in vitro* binding affinity at D1 and D2 receptors, Eur. J. Med. Chem. 27 (1992) 407-411.

[16] H.S. Snyder, *Drugs and the Brain*, Scientific American Library: New York, 1986.

[17] Y. Ando, E. Fuse, W.D. Figg, Thalidomide metabolism by the CYP2C subfamily, Clin. Cancer Res. 8 (2002) 1964-1973.

[18] C. Freiberg, H.P. Fischer, N.A. Brunner, Discovering the mechanism of action of novel antibacterial agents through transcriptional profiling of conditional mutants Antimicrob. Agents Chemother. 49 (2005) 749-759.

[19] C. Freiberg, N.A. Brunner, G. Schiffer, T. Lampe, J. Pohlmann, M. Brands, M. Raabe, D. HaËbich, K. Ziegelbauer, Identification and characterization of the first class of potent bacterial acetyl-CoA carboxylase inhibitors with antibacterial activity, J. Biol. Chem., 279 (2004) 26066-26073.

[20] M. Isaka, N. Rugseree, P. Maithip, P. Kongsaeree, S. Prabpai, Y. Thebtaranonth, Hirsutellones A–E, antimycobacterial alkaloids from the insect pathogenic fungus *Hirsutella nivea* BCC 2594, Tetrahedron 61 (2005) 5577-5583.

[21] S. Chanda, Y. Baravalia, S. Baluja, Synthesis and antibacterial activity of some new triazole derivatives, Arch. Apll. Sci. Res. 2 (2010) 117-126.

[22] (a). H. Bayrak, A. Demirbas, N. Demirbas, S. A. Karaoglu, Synthesis of some new 1,2,4-triazoles starting from isonicotinic acid hydrazide and evaluation of their antimicrobial activities, Eur. J. Med. Chem. 44 (2009) 4362-4366; (b). N.U. Guzeldemirci, O. Kucukbasmaci, Synthesis and antimicrobial activity evaluation of new 1,2,4-triazoles and 1,3,4-thiadiazoles bearing imidazo[2,1-b]thiazole moiety, Eur. J. Med. Chem. 45 (2010) 63-68.

[23] A. Ozdemir, G. Turan-Zitouni, Z.A. Kaplancikli, P. Chevallet, Synthesis of some 4-arylidenamino-4H-1,2,4-triazole-3-thiols and their antituberculosis activity, J. Enzyme Inhib. Med. Chem. 22 (2007) 511-516.

[24] T. Matviiuk, M. Gorichko, C. Lherbet, M. Baltas, Z. Voitenko, Carbon-carbon and carbon-heteroatom conjugate addition of *N*-substituted maleimides to 4H-1,2,4-triazol-3-thioles, 2-amino-1,3-thiazoles, 1H-imidazole and 2-phenylindolizine catalyzed by Lewis acids, J. Org. Pharm. Chem. 11, 3 (2013) 36-42.

[25] X. He, A. Alian, P.R. Ortiz de Montellano, Inhibition of the Mycobacterium tuberculosis enoyl acyl carrier protein reductase InhA by arylamides, Bioorg. Med. Chem. 15 (2007) 6649-6658.

[26] M.R. Kuo, H.R. Morbidoni, D. Alland, S.F. Sneddon, B.B. Gourlie, M.M. Staveski, M. Leonard, J.S. Gregory, A.D. Janjigian, C. Yee, J.M. Musser, B. Kreiswirth, H. Iwamoto, R. Perozzo, W.R. Jacobs Jr., J.C. Sacchettini, D. A. Fidock, Targeting tuberculosis and malaria through inhibition of Enoyl reductase: compound activity and structural data, J. Biol. Chem. 278 (2003) 20851-20859.

[27] (a) X.-H. Liu, J. Zhu, A.-N. Zhou, B.-A. Song, H.-L. Zhu, L.-S. Bai, P. S. Bhadury, C.-X. Pan, Synthesis, structure and antibacterial activity of new 2-(1-(2-(substituted-phenyl)-5-methyloxazol-4-yl)-3-(2-substitued-phenyl)-4,5-dihydro-1H-pyrazol-5-yl)-7-substitued-1,2,3,4-tetrahydroisoquinoline derivatives, Bioorg. Med. Chem. 17 (2009) 1207-1213. (b) R.K. Tiwari, D. Singh, J. Singh, A.K. Chhillar, R. Chandra, A.K. Verma, Synthesis, antibacterial activity and QSAR studies of 1,2-disubstituted-6,7-dimethoxy-1,2,3,4-tetrahydroisoquinolines, Eur. J. Med. Chem. 41 (2006) 40-49.

[28] P. Kumar, K.N. Dhawan, K. Kishore, K.P. Bhargava, 1-Phenyl-6,7-disubstituted-aminopropyl)-1,2,3,4-tetrahydroisoquinolines as possible antituberculer agents. J. Heterocycl. Chem. 19 (1982) 677-679.

[29] K. Iwasa, M. Moriyasu, Y. Tachibana, H. Kim, Y Wataya, W Wiegrebe, K. F. Bastowm L. M. Cosentio, M. Kozuka, K. Lee, Simple isoquinoline and benzylisoquinoline alkaloids as potential antimicrobial, antimalarial, cytotoxic, and anti-HIV agents. Bioorg. Med. Chem. 9 (2001) 2871-2884.

[30] M. B. Hansen, S. E. Nielsen, K. Berg, Re-examination and further development of a precise and rapid dye method for measuring cell growth/cell kill. J. Immunol. Methods 119 (1989) 203-210.

[31] R. Gomez-Flores, S. Gupta, R. Tamez-Guerra, R. T. Mehta, Determination of MICs for Mycobacterium avium-M. intracellulare complex in liquid medium by a colorimetric method. J. Clin. Microbiol. 33 (1995) 1842-1846.

[32] (a) C. Menendez, S. Gau, C. Lherbet, F. Rodriguez, C. Inard, M.R. Pasca, M. Baltas, Synthesis and biological activities of triazole derivatives as inhibitors of InhA and antituberculosis agents, Eur. J. Med. Chem. 46 (2011) 5524-5531; (b) C. Menendez, A. Chollet, F. Rodriguez, C. Inard, M.R. Pasca, C. Lherbet, M. Baltas, Chemical synthesis and biological evaluation of triazole derivatives as inhibitors of InhA and antituberculosis agents, Eur. J. Med. Chem. 52 (2012) 275-283.

[33] S.L. Parikh, G. Xiao, P.J. Tonge, Inhibition of InhA, the enoyl reductase from Mycobacterium tuberculosis, by triclosan and isoniazid, Biochemistry 39 (2000) 7645-7650.

[34] X. He, A. Alian, P. R. Ortiz de Montellano, Inhibition of the Mycobacterium tuberculosis enoyl acyl carrier protein reductase InhA by arylamides, Bioorg. Med. Chem. 15 (2007) 6649-6658.

[35] E. Pohjala, A facile synthesis of stable dihydroindolizines via intramolecular 1,5-cyclization of ylides, Tetrahedron Lett. 25 (1972) 2585-2588.

[36] W. Augstein, F. Kroehnke, Synthesen des Benzo[*a*]- und des Naphtho[2.3-*b*]indolizin-Ringsystems, Justus Liebigs Annalen der Chemie, 697 (1966) 158-170.

[37] H.M. Berman, J. Westbrook, Z. Feng, G. Gilliland, T. N. Bhat, H. Weissig, I. N. Shindyalov, P. E. Bourne, The Protein Data Bank, Nucl. Acids Res. 28 (2000) 235-242 (www.pdb.org).

[38] R. Thomsen, M. H. Christensen, MolDock: A new technique for high-accuracy molecular docking, J. Med. Chem. 49 (2006) 3315-3321.

[39] O. Korb, T. Stützle, T. E. Exner, Empirical Scoring Functions for Advanced Protein-Ligand Docking with PLANTS, J. Chem. Inf. Model. 49 (2009) 84-96.

Table 1. Yields determined for each compound.

Cpd	R	Yield (%)
2a	Ph	62
2b	*p*-MeO-C_6H_4	63
4a	Ph	88 (Method A) 70 (Method B)
4b	Bn	83 (Method A) 58 (Method B)
6a	Ph	87 (Method A) 55 (Method B)
6b	Bn	79 (Method A) 60 (Method B)
8a	Ph	95
8b	*p*-MeO-C_6H_4	92
11a	Ph	84
11b	Bn	71
12	Ph	62

Table 2. Yields of the synthesized compounds; InhA inhibition values; Minimal Inhibitory Concentration (MIC) values; Cytotoxicities.

Cpd	R	% Inhibition at 50 µM[a]	MIC[b] (µg/ml) / (µM)	Cytotoxicity IC_{50} (µM) HCT116/GM637H
2a	Ph	15	5 / 18.2	17 / 15
2b	*p*-MeO-C_6H_4	22	5 / 16.4	ND
4a	Ph	52	40 / 94.4	>100 / > 100
4b	Bn	56	40 / 91.4	ND
6a	Ph	20	2.5 / 8.2	>100 / >100
6b	Bn	16	10 / 31.2	>100 / >100
8a	Ph	9	20 / 82.9	>100 / >100
8b	*p*-MeO-C_6H_4	21	15 / 55.3	ND
11a	Ph	22	40 / 109.2	>100 / >100
11b	Bn	12	20 / 52.6	ND
12	Ph	45	20 / 46.5	>100 / >100
Triclosan		>99	10 / 34.5	ND
Isoniazid		---	0.05/0.4	ND
GEQ		>99	>125 / >317.7	ND

[a] The results are expressed as a percentage of InhA inhibition.
[b] Minimal inhibitory concentration on *M. tuberculosis* H37Rv strain

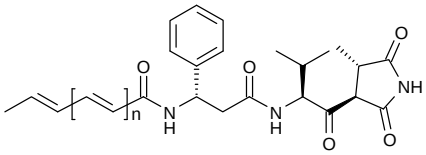

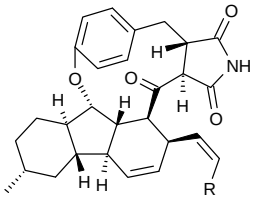

Fig. 1. Structures of natural antibiotics (Miroamide B and Andrimid) and antimycobacterial alkaloids Hirsutellone A and D bearing succinimide fragments.

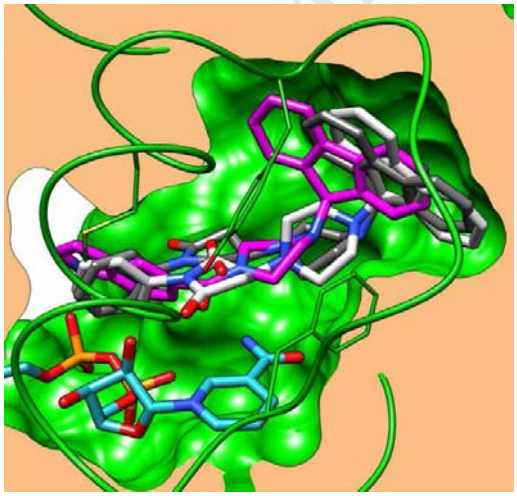

Fig. 2. Superposition of GEQ crystallographic bindings (carbons colored in magneta; 1P44 pdb entry) and predicted binding modes of **4a**; *R*-enantiomer U5A (dark grey) and *S*-enantiomer D5A (light grey).

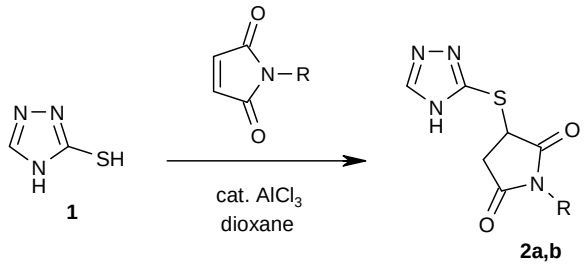

1 **2a,b**

Scheme 1. Catalytic conjugate addition of maleimides to 4*H*-1,2,4-triazole-3-thiole **1**. **2a** R = Ph; **2b** R = *p*-CH_3O-C_6H_4.

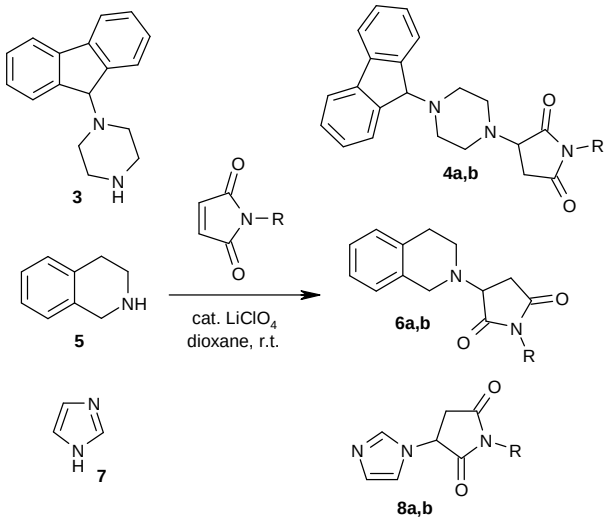

3 **4a,b** **5** **6a,b** **7** **8a,b**

Scheme 2. Synthesis of C–N Michael adducts. **4a**, **6a**, **8a** R = Ph; **4b**, **6b** R = Bn; **8b** R = *p*-CH_3O-C_6H_4.

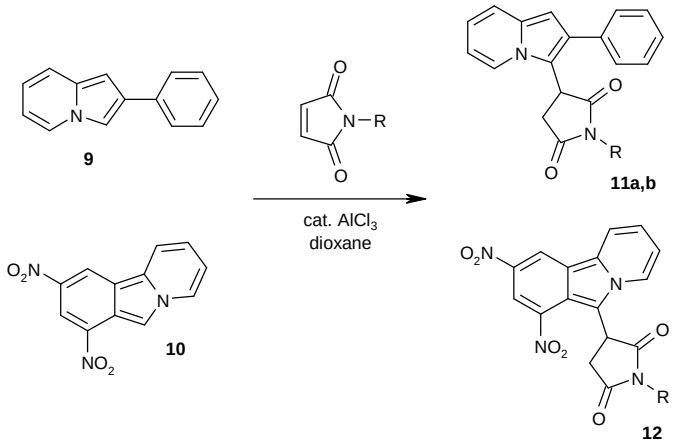

Scheme 3. Catalytic conjugate addition of *N*-substituted maleimides to 2-phenylindolizine (**9**) and 7,9-dinitropyrido[2,1-a]isoindole (**10**). **11a**, **12** R = Ph; **11b** R = Bn.

- A series of 3-heteryl substituted pyrrolidine-2,5-dione were synthesized.
- They displayed promising inhibitory activity against *M. tuberculosis* H37Rv.
- Some of them present inhibition activities against InhA.

Synthesis of 3-heteryl substituted pyrrolidine-2,5-diones *via* catalytic Michael reaction and evaluation of their inhibitory activity against InhA and *Mycobacterium tuberculosis*

Tetiana Matviiuk,[a,b] Giorgia Mori,[d] Christian Lherbet,*[,a,c] Marian Gorichko,[b] Frédéric Rodriguez,[a,c] Maria Rosalia Pasca,[d] Brigitte Guidetti,[a,c] Zoia Voitenko,*[a,b] Michel Baltas*[a,c]

Supplementary information

I. NMR spectra for the compounds

II. Inhibition values

III. Cytotoxicities of the compounds

IV. Molecular docking studies

I. NMR spectra of the compounds

Compound 2a

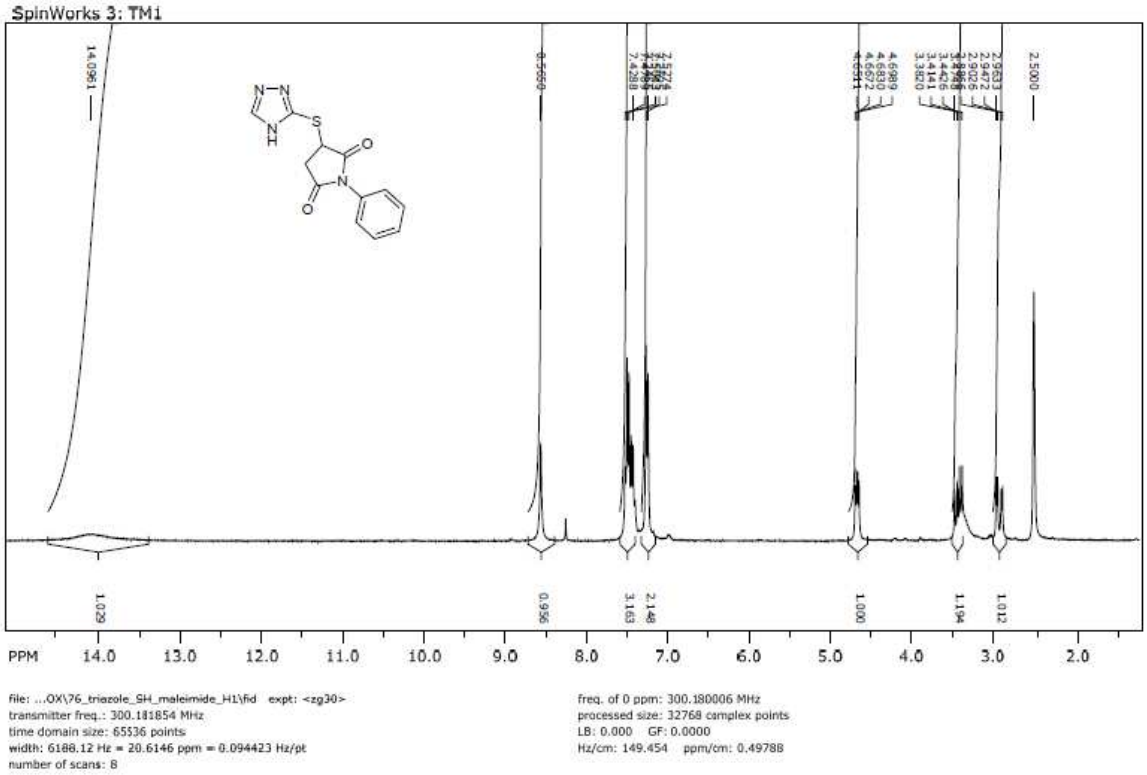

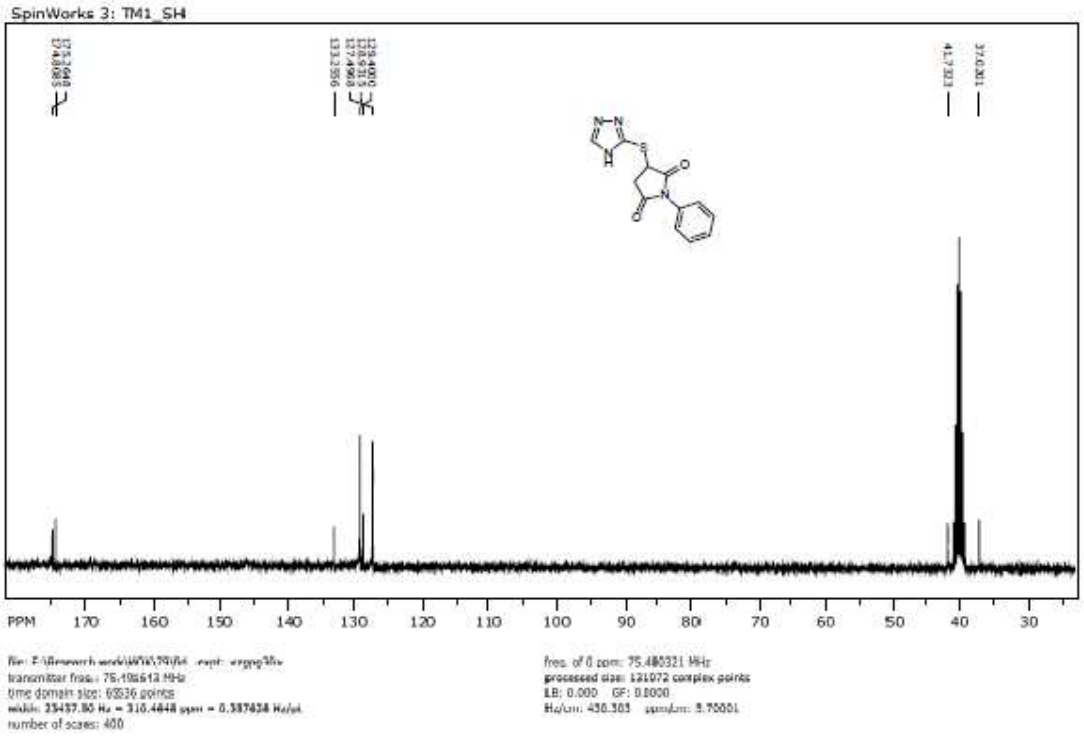

Compound 2b:

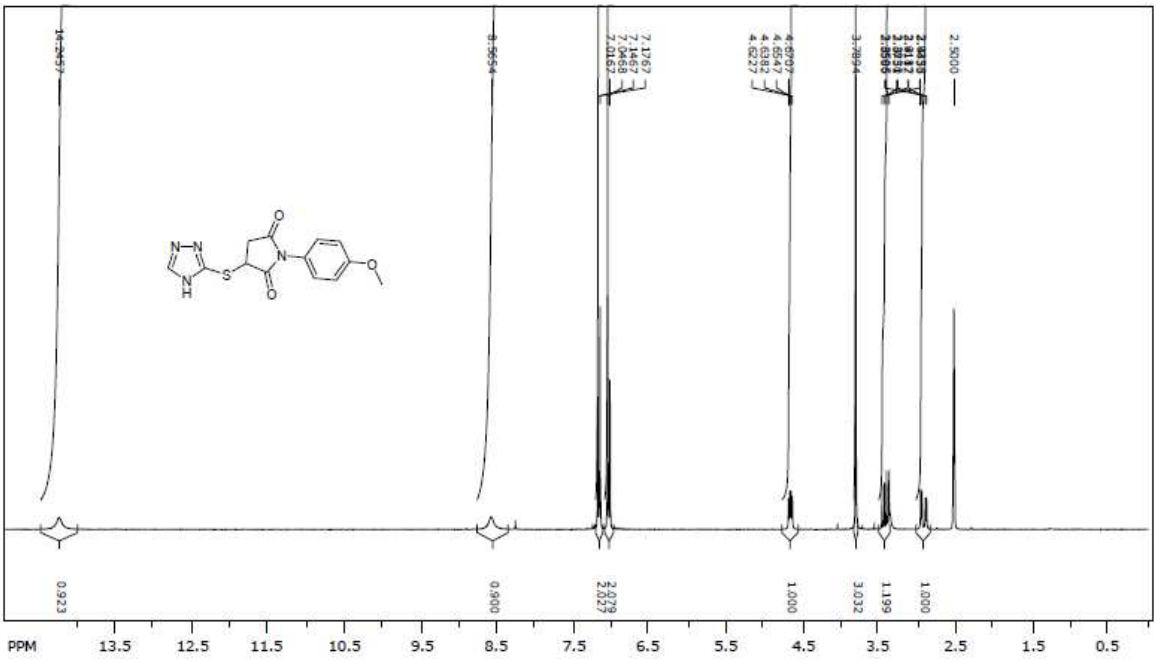

file: ... work\MOX\78_triazole_SCOMe_H1\fid expt: <zg30>
transmitter freq.: 300.181854 MHz
time domain size: 65536 points
width: 6188.12 Hz = 20.6146 ppm = 0.094423 Hz/pt
number of scans: 16

freq. of 0 ppm: 300.180006 MHz
processed size: 32768 complex points
LB: 0.000 GF: 0.0000
Hz/cm: 161.053 ppm/cm: 0.53652

SpinWorks 3: TM2_SCOMe

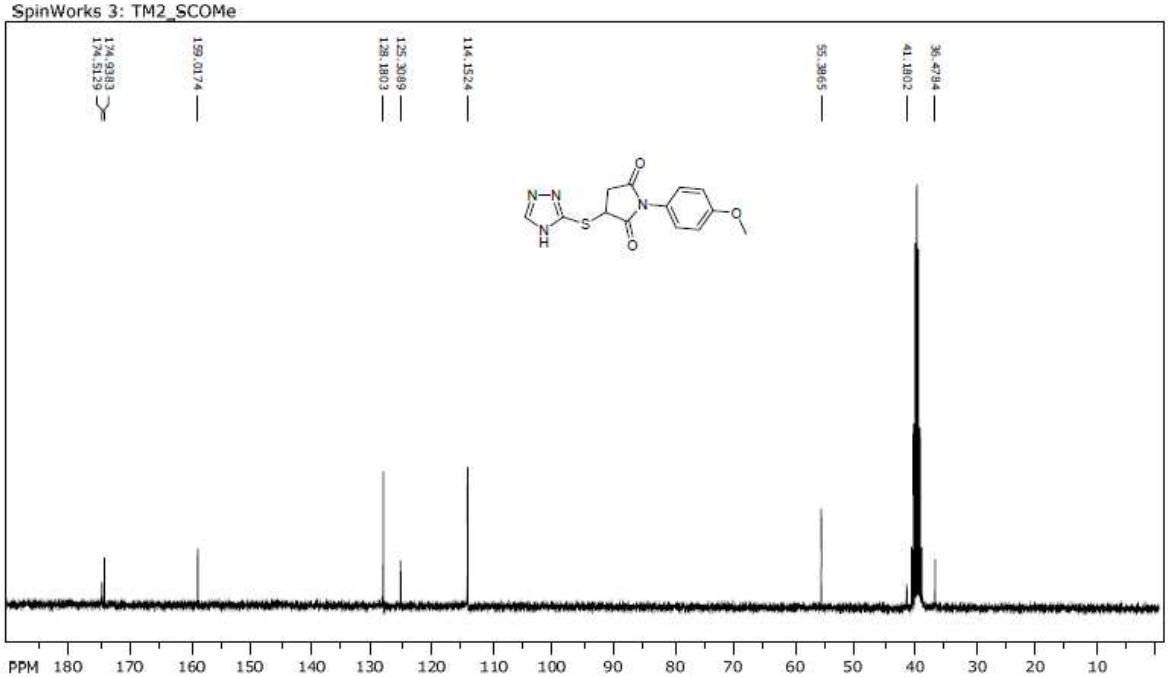

file: ...work\MOX\77_triazole_SCOMe_C13\fid expt: <zgpg30>
transmitter freq.: 75.491643 MHz
time domain size: 65536 points
width: 23437.50 Hz = 310.4648 ppm = 0.357628 Hz/pt
number of scans: 800

freq. of 0 ppm: 75.480356 MHz
processed size: 131072 complex points
LB: 0.000 GF: 0.0000
Hz/cm: 516.600 ppm/cm: 6.84225

Compound 4a:

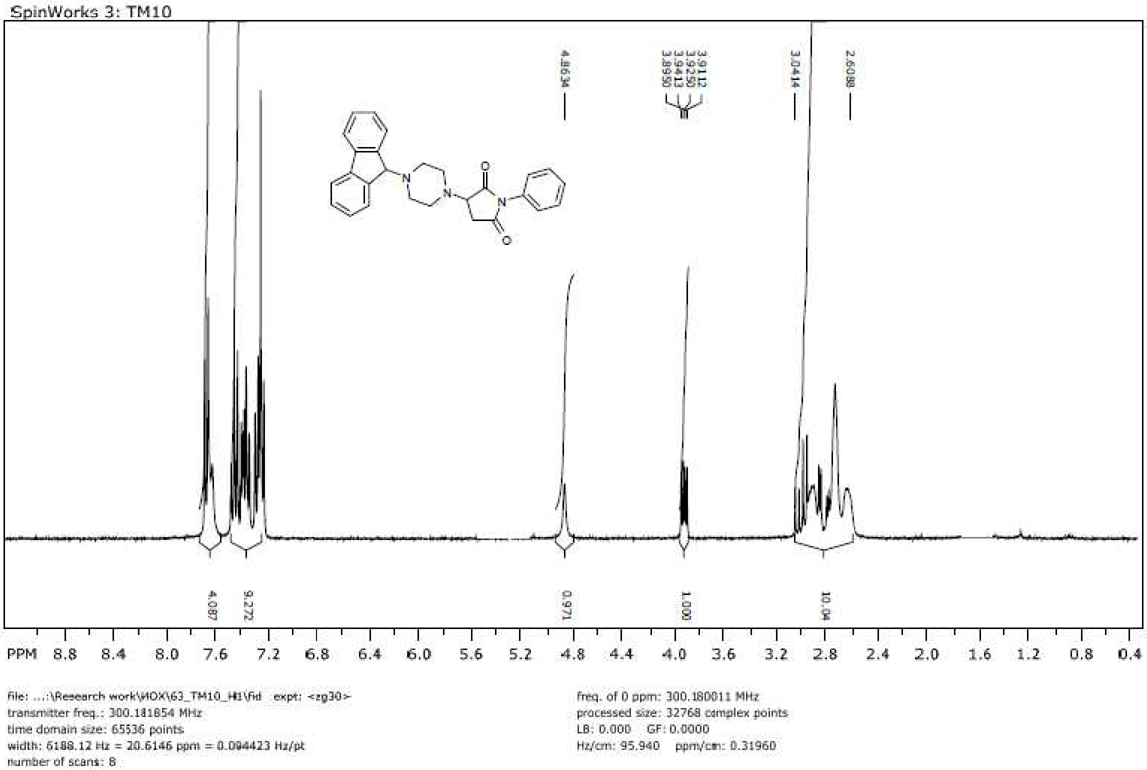
SpinWorks 3: TM10
4.8634
3.9112
3.9250
3.9413
3.8950
3.0414
2.6088
4.087
9.272
0.971
1.000
10.04
PPM 8.8 8.4 8.0 7.6 7.2 6.8 6.4 6.0 5.6 5.2 4.8 4.4 4.0 3.6 3.2 2.8 2.4 2.0 1.6 1.2 0.8 0.4
file: ...:\Research work\MOX\63_TM10_H1\fid expt: <zg30>
transmitter freq.: 300.181854 MHz
time domain size: 65536 points
width: 6188.12 Hz = 20.6146 ppm = 0.094423 Hz/pt
number of scans: 8
freq. of 0 ppm: 300.180011 MHz
processed size: 32768 complex points
LB: 0.000 GF: 0.0000
Hz/cm: 95.940 ppm/cm: 0.31960

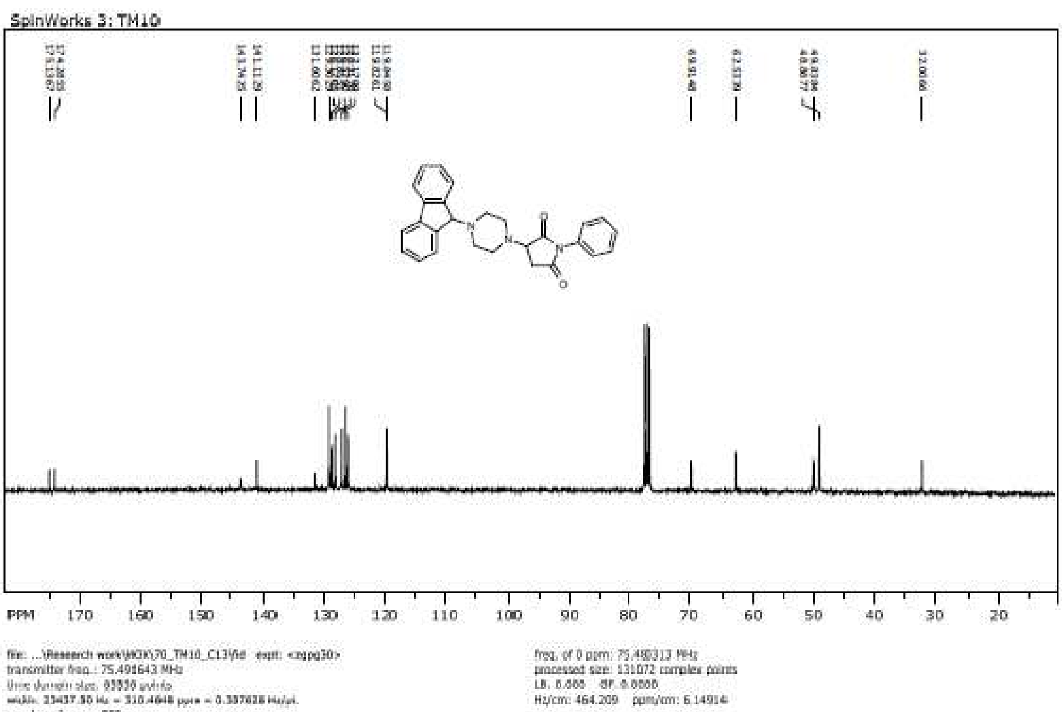
SpinWorks 3: TM10
PPM 170 160 150 140 130 120 110 100 90 80 70 60 50 40 30 20
transmitter freq.: 75.491643 MHz
freq. of 0 ppm: 75.480313 MHz
processed size: 131072 complex points
Hz/cm: 464.209 ppm/cm: 6.14914

Compound 4b:

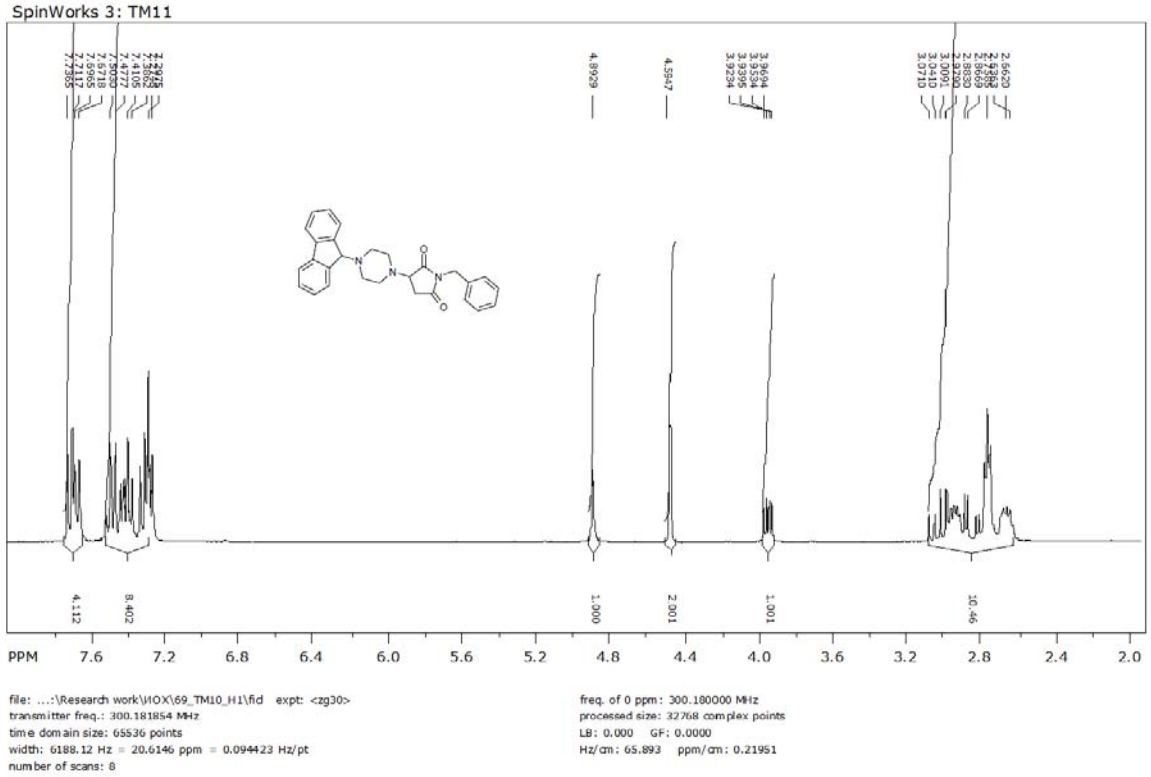

Compound 6a:

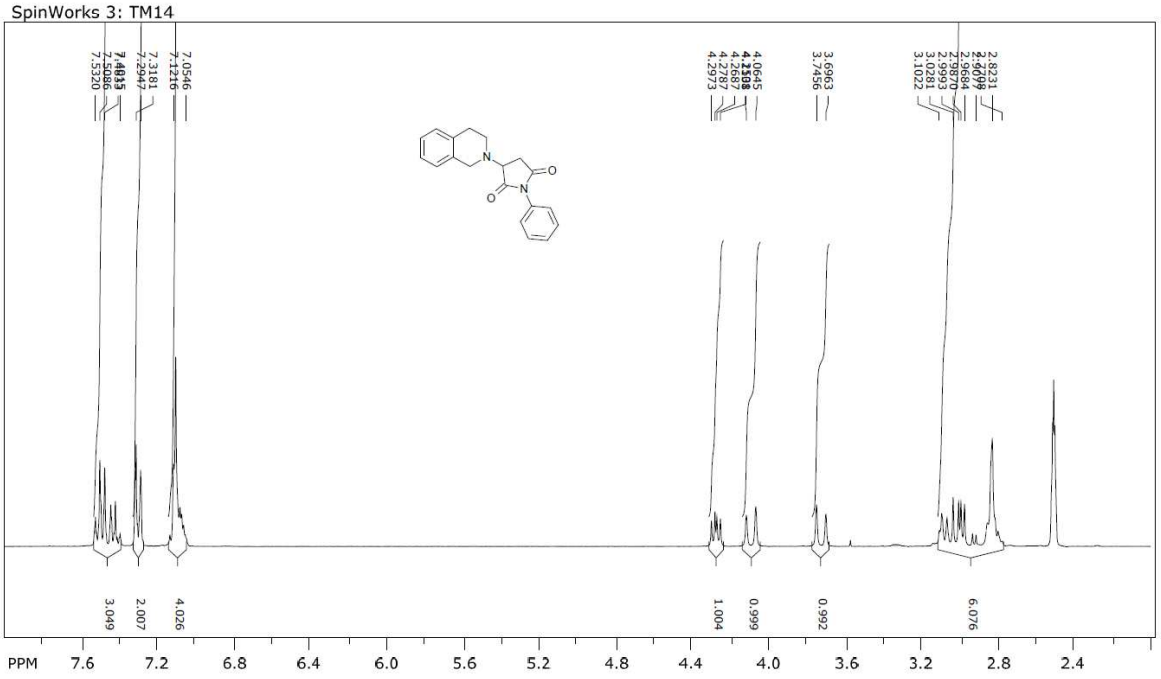

file: ...:\Research work\HOX\55_TM14_H1\fid expt: <zg30>
transmitter freq.: 300.181854 MHz
time domain size: 65536 points
width: 6188.12 Hz = 20.6146 ppm = 0.094423 Hz/pt
number of scans: 8

freq. of 0 ppm: 300.180006 MHz
processed size: 32768 complex points
LB: 0.000 GF: 0.0000
Hz/cm: 64.526 ppm/cm: 0.21496

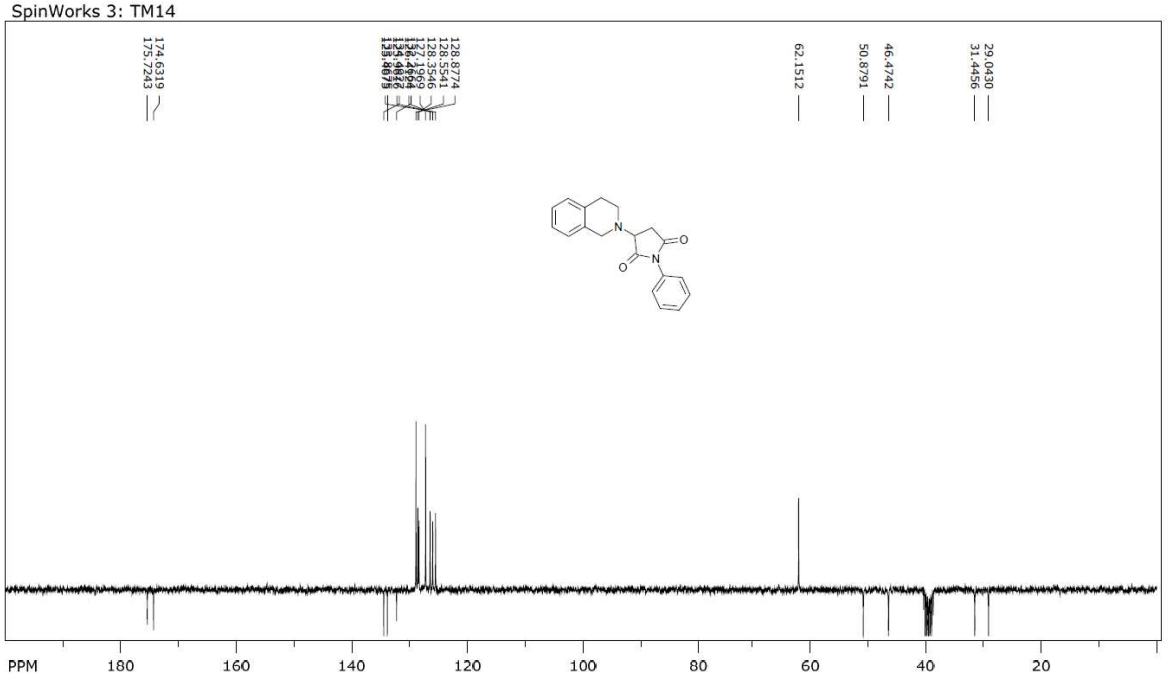

file: ...\Research work\HOX\56_TM14_C13\fid expt: <jmod>
transmitter freq.: 75.487869 MHz
time domain size: 65536 points
width: 22727.27 Hz = 301.0719 ppm = 0.346791 Hz/pt
number of scans: 256

freq. of 0 ppm: 75.480357 MHz
processed size: 131072 complex points
LB: 0.000 GF: 0.0000
Hz/cm: 541.343 ppm/cm: 7.17125

Compound 6b:

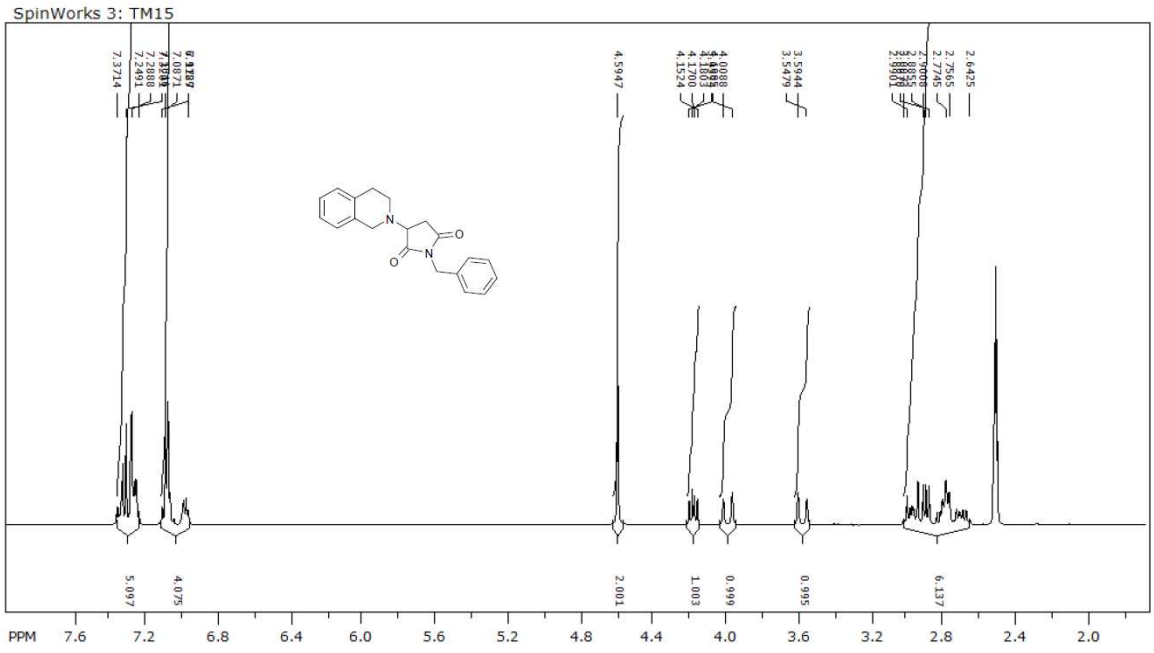
SpinWorks 3: TM15
7.3714
7.2491
7.2288
7.1087
7.0871
4.5947
4.1524
4.1700
3.5944
3.5479
2.7745
2.7565
2.6425
5.097
4.075
2.001
1.003
0.999
0.995
6.137
PPM 7.6 7.2 6.8 6.4 6.0 5.6 5.2 4.8 4.4 4.0 3.6 3.2 2.8 2.4 2.0
file: ...:\Research work\MOX\57_TM15_H1\fid expt: <zg30>
transmitter freq.: 300.181854 MHz
time domain size: 65536 points
width: 6188.12 Hz = 20.6146 ppm = 0.094423 Hz/pt
number of scans: 8
freq. of 0 ppm: 300.180006 MHz
processed size: 32768 complex points
LB: 0.000 GF: 0.0000
Hz/cm: 67.745 ppm/cm: 0.22568

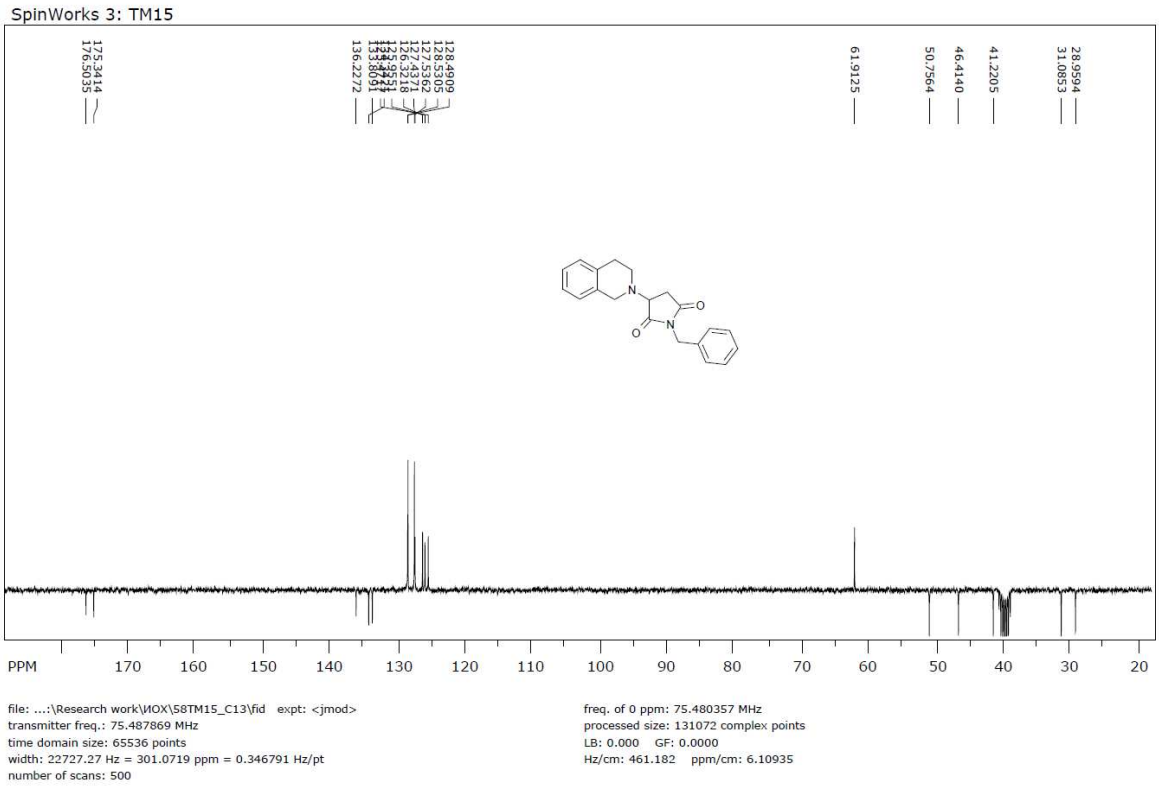
SpinWorks 3: TM15
175.3414
176.5035
136.2272
128.4909
61.9125
50.7564
46.4140
41.2205
28.9594
31.0853
PPM 170 160 150 140 130 120 110 100 90 80 70 60 50 40 30 20
file: ...:\Research work\MOX\58TM15_C13\fid expt: <jmod>
transmitter freq.: 75.487869 MHz
time domain size: 65536 points
width: 22727.27 Hz = 301.0719 ppm = 0.346791 Hz/pt
number of scans: 500
freq. of 0 ppm: 75.480357 MHz
processed size: 131072 complex points
LB: 0.000 GF: 0.0000
Hz/cm: 461.182 ppm/cm: 6.10935

Compound 8a:

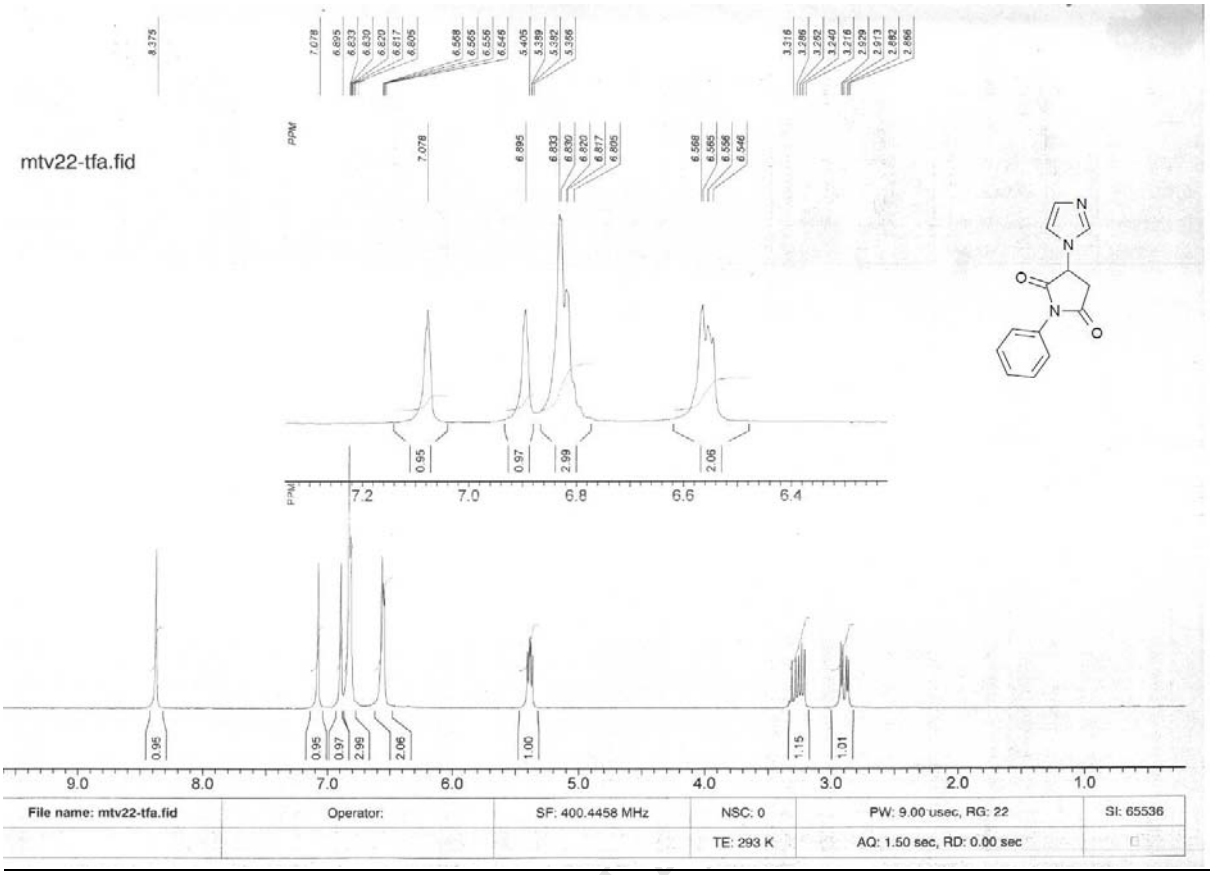

Compound 8b:

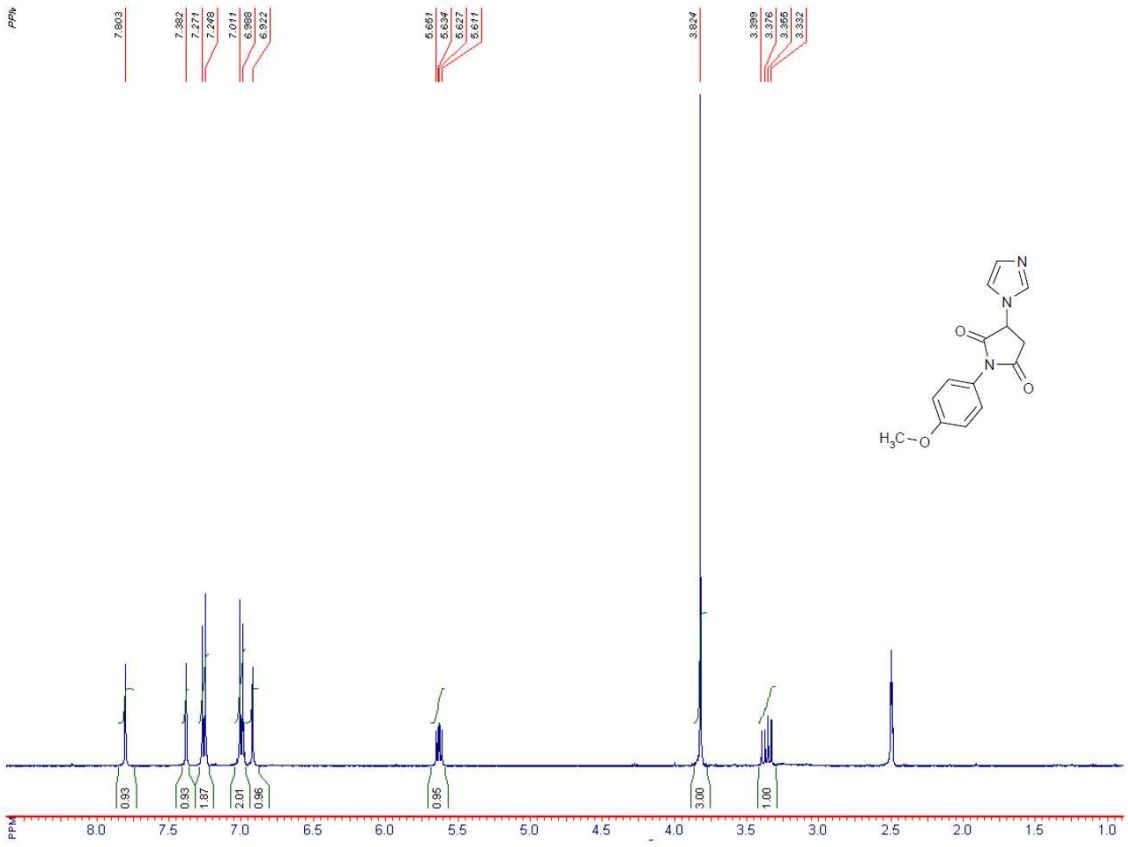

Compounds 11a:

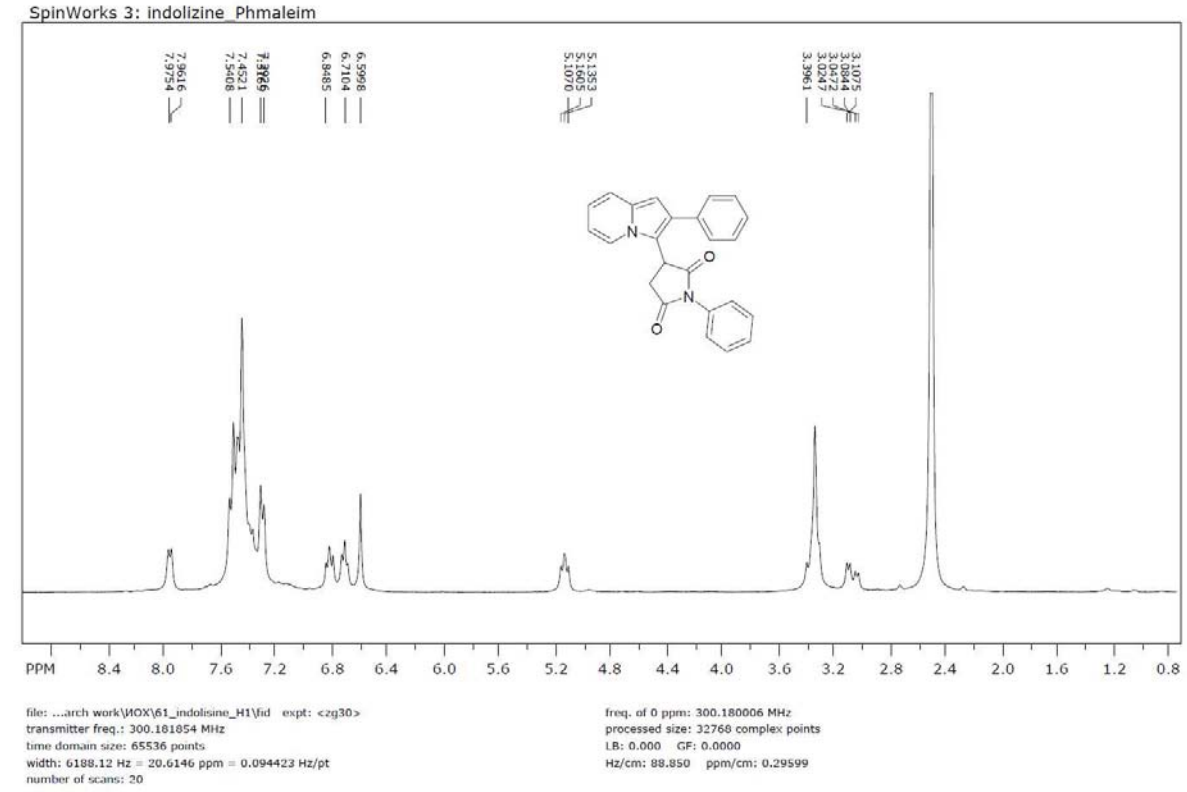

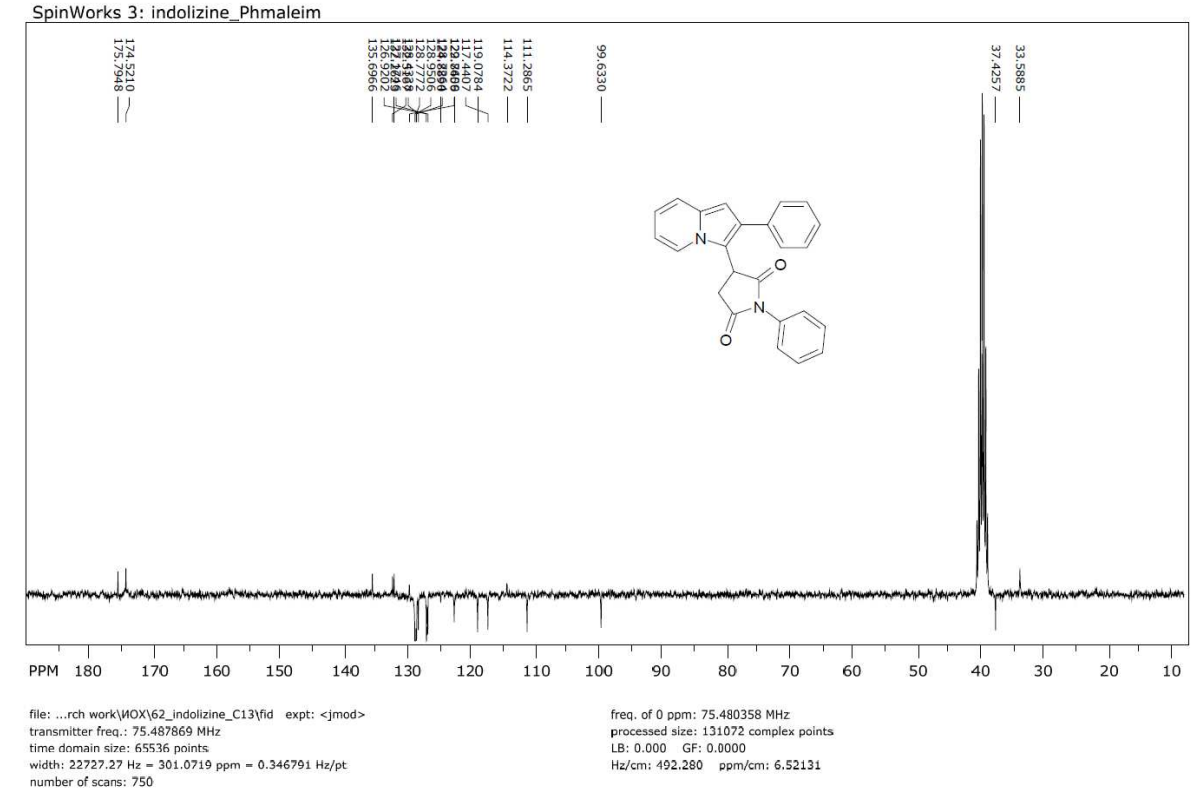

Compounds 11b:

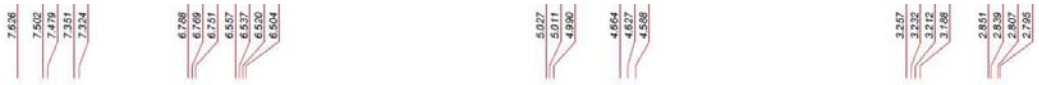

M_M.fid

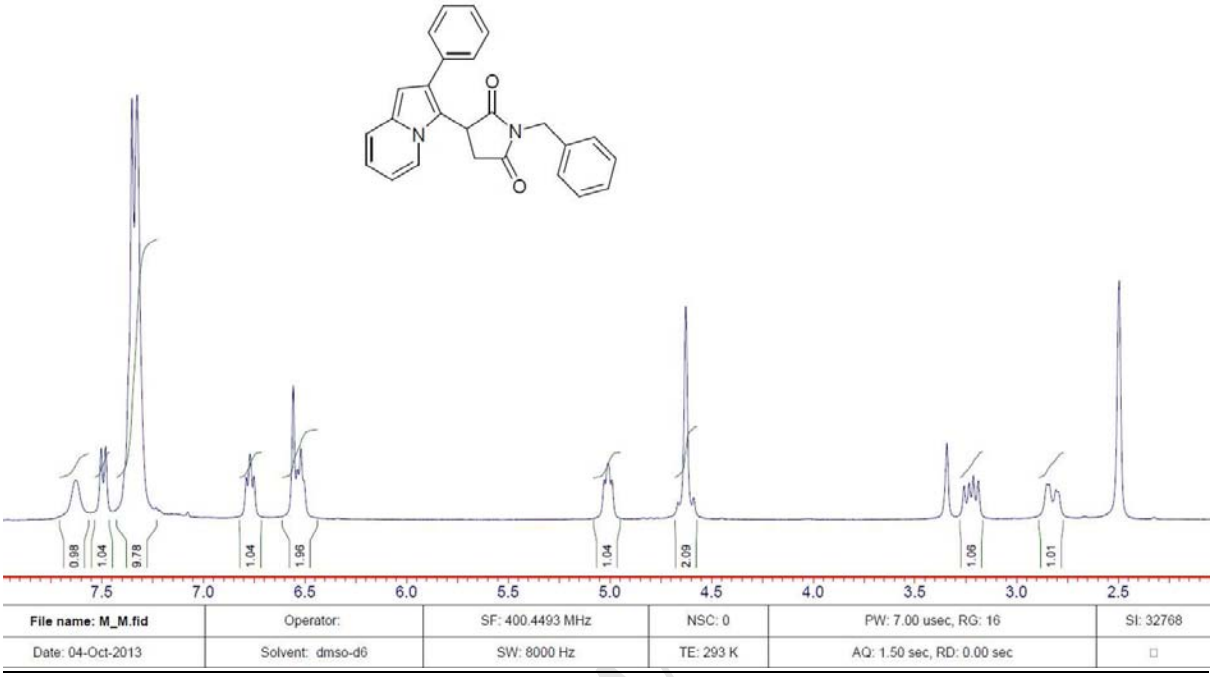

File name: M_M.fid	Operator:	SF: 400.4493 MHz	NSC: 0	PW: 7.00 usec, RG: 16	SI: 32768
Date: 04-Oct-2013	Solvent: dmso-d6	SW: 8000 Hz	TE: 293 K	AQ: 1.50 sec, RD: 0.00 sec	□

M-M-C13.fid

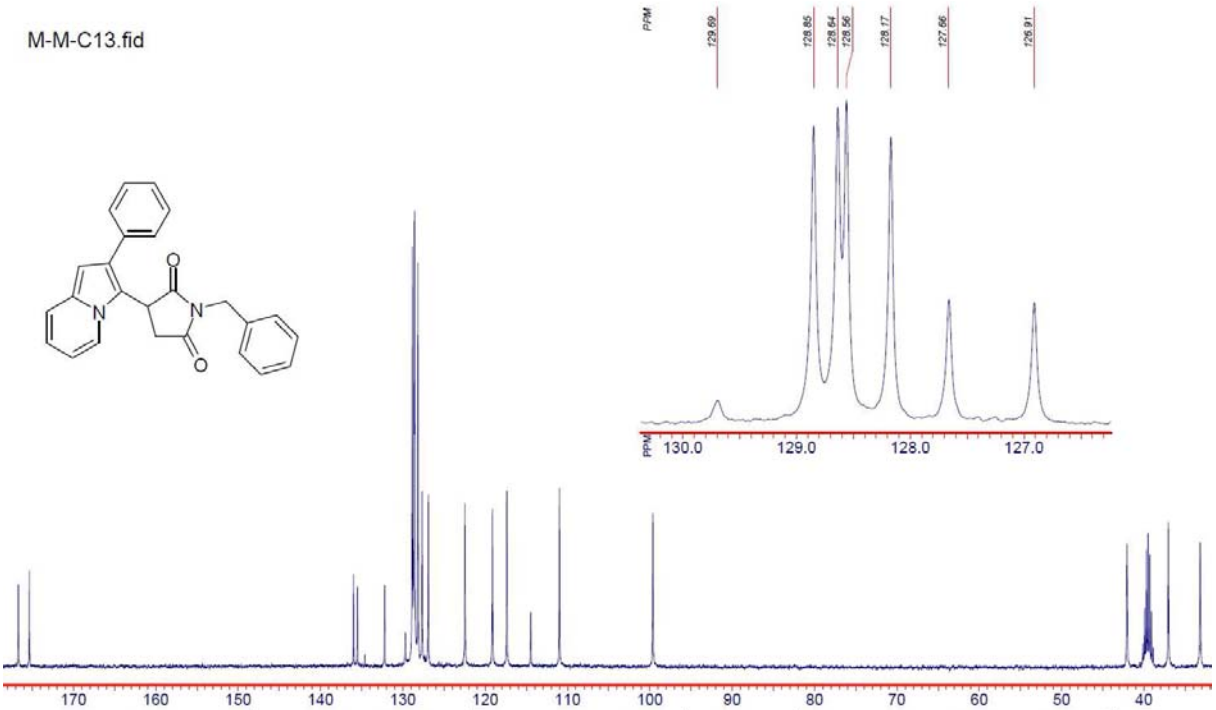

File name: M-M-C13.fid	Operator:	SF: 100.7035 MHz	NSC: 0	PW: 8.50 usec, RG: 34	SI: 262144
Date: 04-Oct-2013	Solvent: DMSO-d6	SW: 27701 Hz	TE: 293 K	AQ: 1.20 sec, RD: 0.00 sec	□

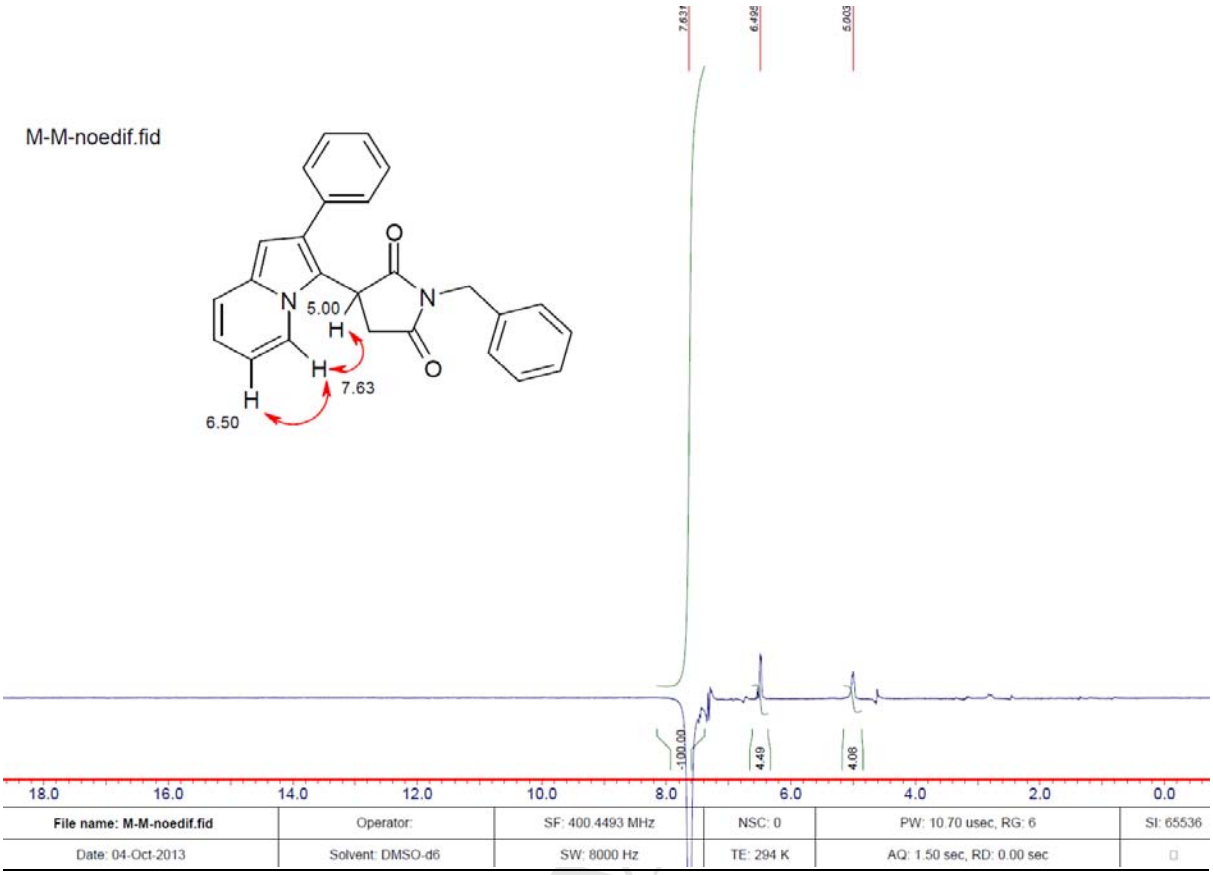
M-M-noedif.fid
5.00
7.63
6.50
7.691
6.498
5.003
100.00
4.49
4.08
18.0
16.0
14.0
12.0
10.0
8.0
6.0
4.0
2.0
0.0
File name: M-M-noedif.fid
Operator:
SF: 400.4493 MHz
NSC: 0
PW: 10.70 usec, RG: 6
SI: 65536
Date: 04-Oct-2013
Solvent: DMSO-d6
SW: 8000 Hz
TE: 294 K
AQ: 1.50 sec, RD: 0.00 sec

Compound 12

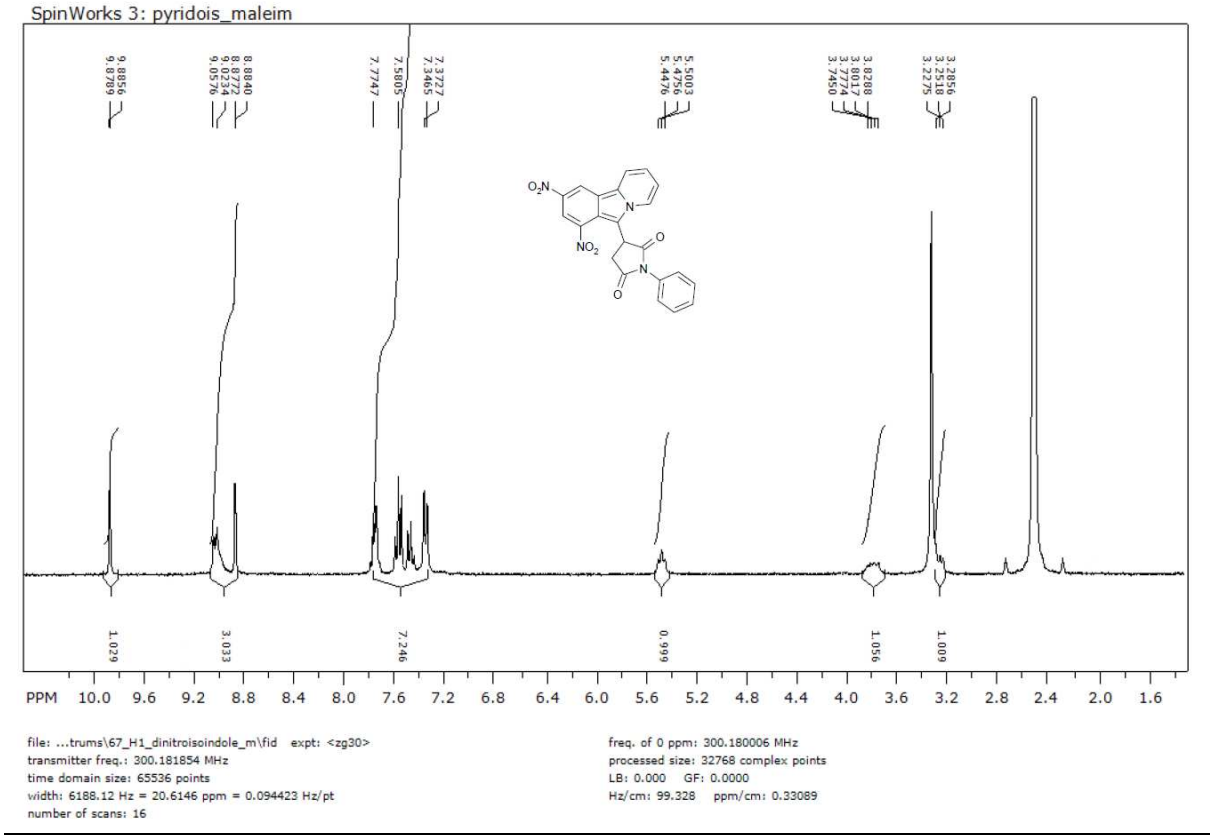
SpinWorks 3: pyridois_maleim
9.8856
9.8789
9.0576
9.0234
8.8840
8.8772
7.7747
7.5805
7.3727
7.3465
5.5003
5.4756
5.4476
3.8288
3.8017
3.7774
3.7450
3.2856
3.2518
3.2275
1.029
3.033
7.246
0.999
1.056
1.009
PPM 10.0 9.6 9.2 8.8 8.4 8.0 7.6 7.2 6.8 6.4 6.0 5.6 5.2 4.8 4.4 4.0 3.6 3.2 2.8 2.4 2.0 1.6
file: ...trums\67_H1_dinitroisoindole_m\fid expt: <zg30>
transmitter freq.: 300.181854 MHz
time domain size: 65536 points
width: 6188.12 Hz = 20.6146 ppm = 0.094423 Hz/pt
number of scans: 16
freq. of 0 ppm: 300.180006 MHz
processed size: 32768 complex points
LB: 0.000 GF: 0.0000
Hz/cm: 99.328 ppm/cm: 0.33089

II. Inhibition values

Cpd	1) % inhibition at (50 µM)	2) % inhibition at (50 µM)	3) % inhibition at (50 µM)	average inhibition % at (50 µM)	Standard deviation
2a	13	15	16	15	2
2b	24	19	23	22	3
4a	52	51	50	52	1
4b	54	57	56	56	2
6a	20	20	19	20	1
6b	15	18	15	16	2
8a	10	9	11	9	1
8b	21	21	20	21	1
11a	20	24	19	21	3
11b	11	11	14	12	2
12	44	46	46	45	1

III.Cytotoxicities of different compounds

Compound 2a:

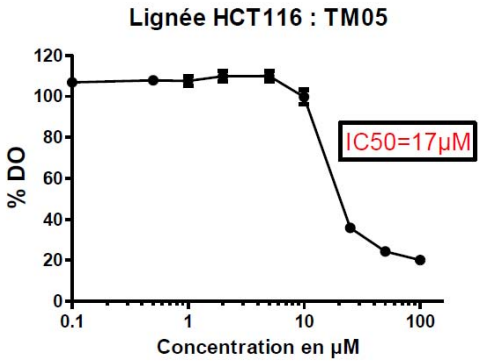

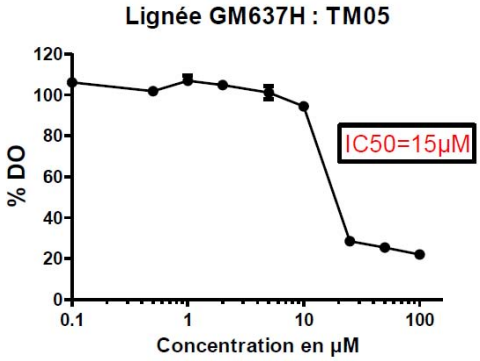

Compound 4a:

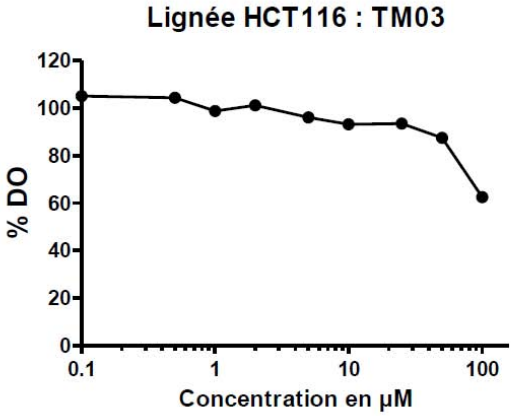

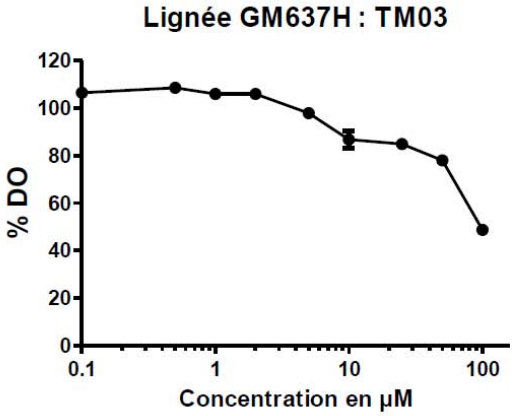

Compound 6a:

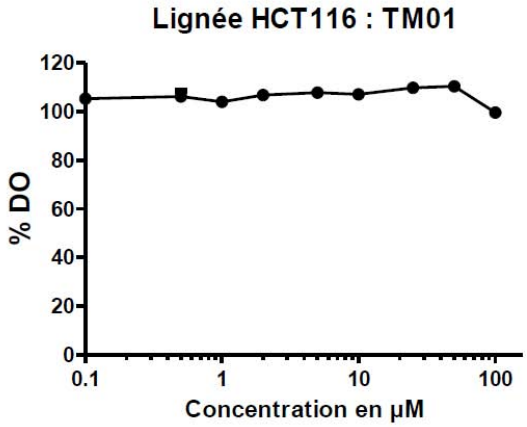

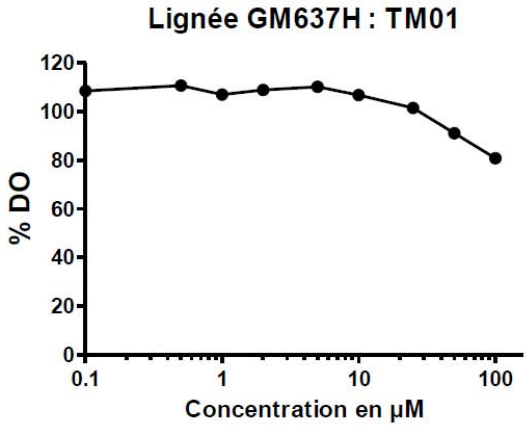

Compound 6b:

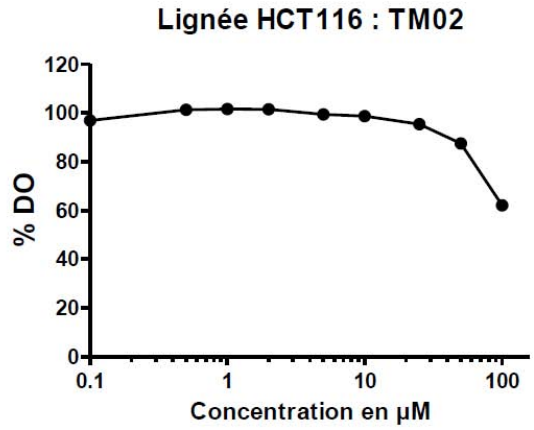

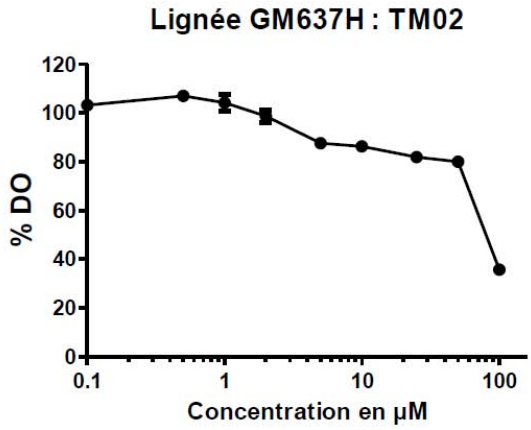

Compound 8a:

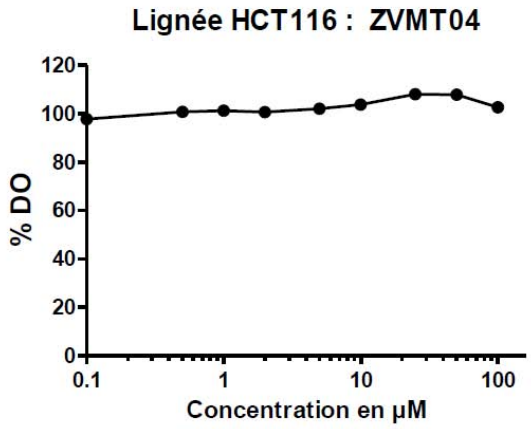

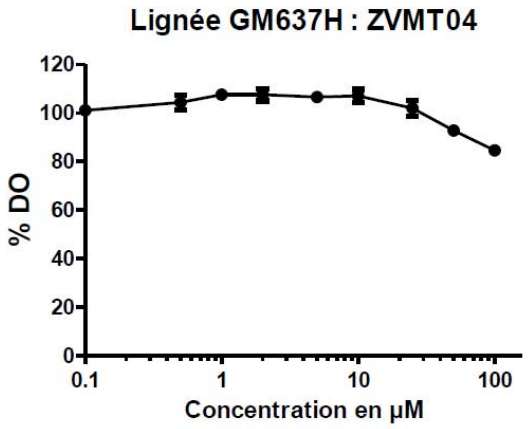

Compound 11a:

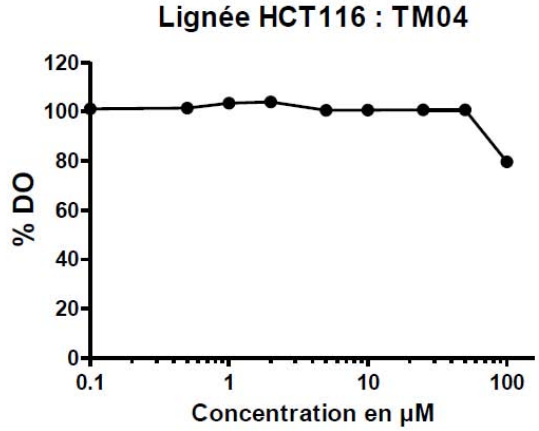

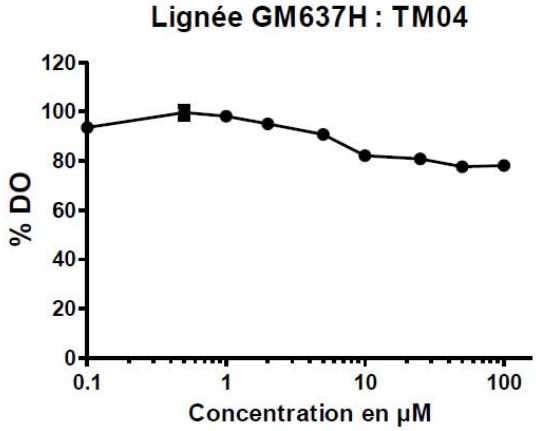

Compound 12:

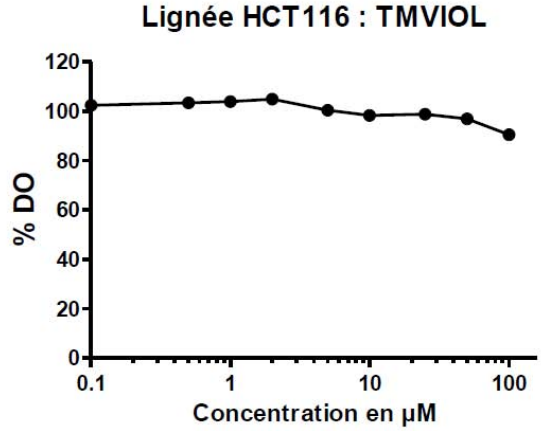

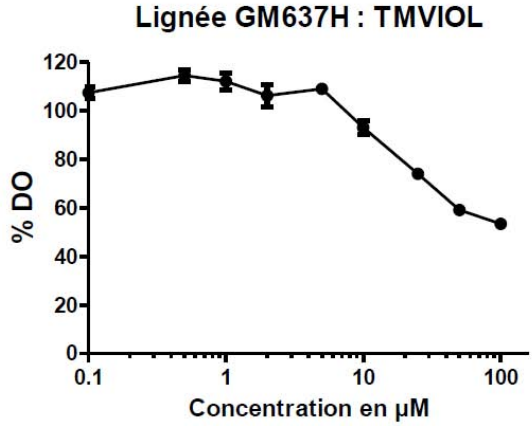

IV. Molecular docking studies

The graph representation of normalized descriptors LE1 (Molegro's Moldock Score divided by heavy atoms number) *vs* LE3 (Molegro's Rerank score divided by heavy atoms number) obtained from the docking studies of compound **4a** (*R*- and *S*-enantiomers) and GEQ (60 calculation runs followed by clustering of results) is shown on **Fig. 1**.

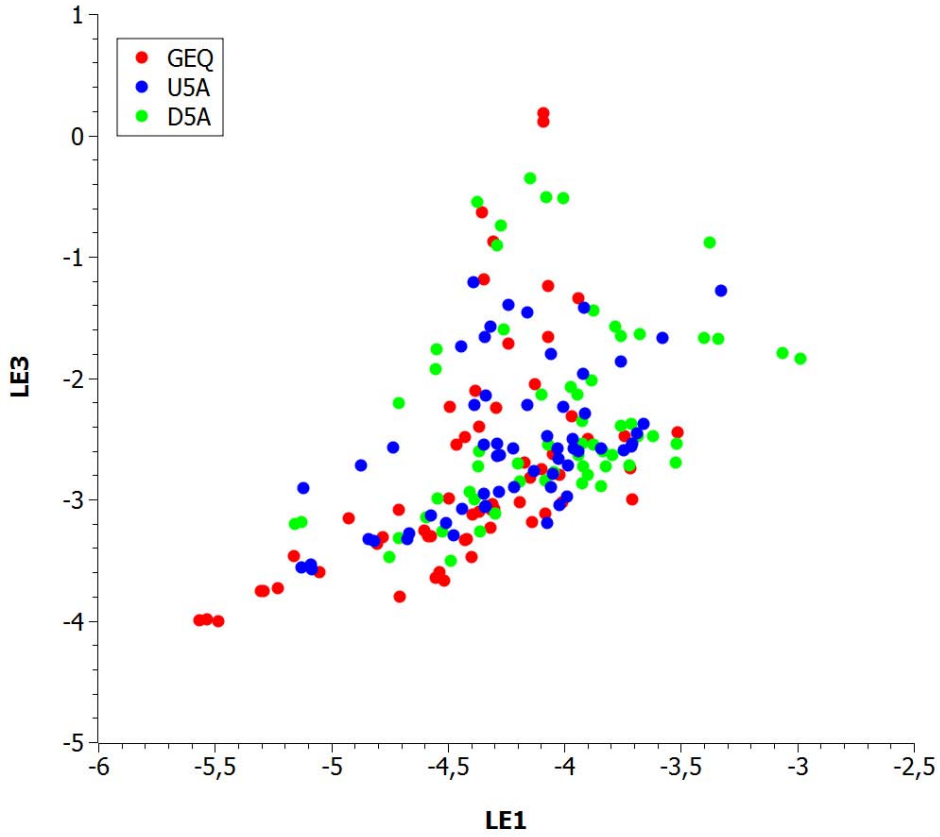

SIFig. 1 Graph of Molegro [*MOLEGRO_2006*] LE3 (Molegro's Rerank score divided by heavy atoms number) *vs* LE1 (Moldock Score divided by heavy atoms number) normalized descriptors for the **GEQ** (red) and compound **4a**, blue: R-enantiomer (U5A); green: S-enantiomer (D5A) (60 calculation runs followed by clustering of results).

The lowest values of LE1 and LE3 descriptors are considered as limit values: after a given number of runs these best values do not evolve and show similar poses (even if initial conditions and optimization method could be different). The graph clearly shows that the best values are significantly related to **GEQ** (in red) (the worst values correspond to poses outside the binding site) rather than compound **4a**. The *R* and *S* enantiomers of compound **4a** does not show significantly different results relative to the descriptors used. These data is in accordance with biological results.

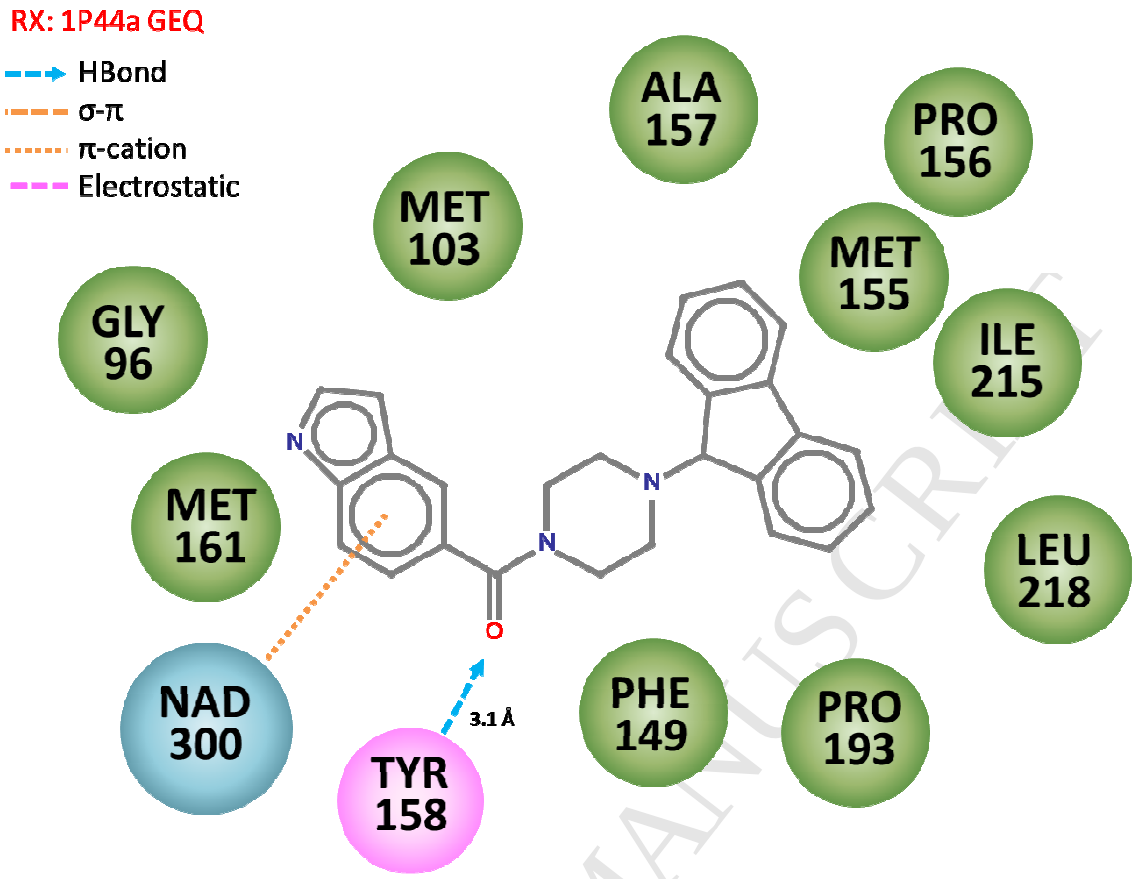

SIFig.2 - 2D ligand-protein interaction diagrams of crystallographic structure 1P44, chain A (1P44a) generated using Accelrys Discovery Studio [*DSV_2005*] and annotated. The canonical set of interactions is composed by PHE149, MET161, MET103, LEU218, ILEU215, ALA157 residues. Other methods (i.e. LigPlot based [*LASKOWSKI_2011*]) for map generation display similar results.

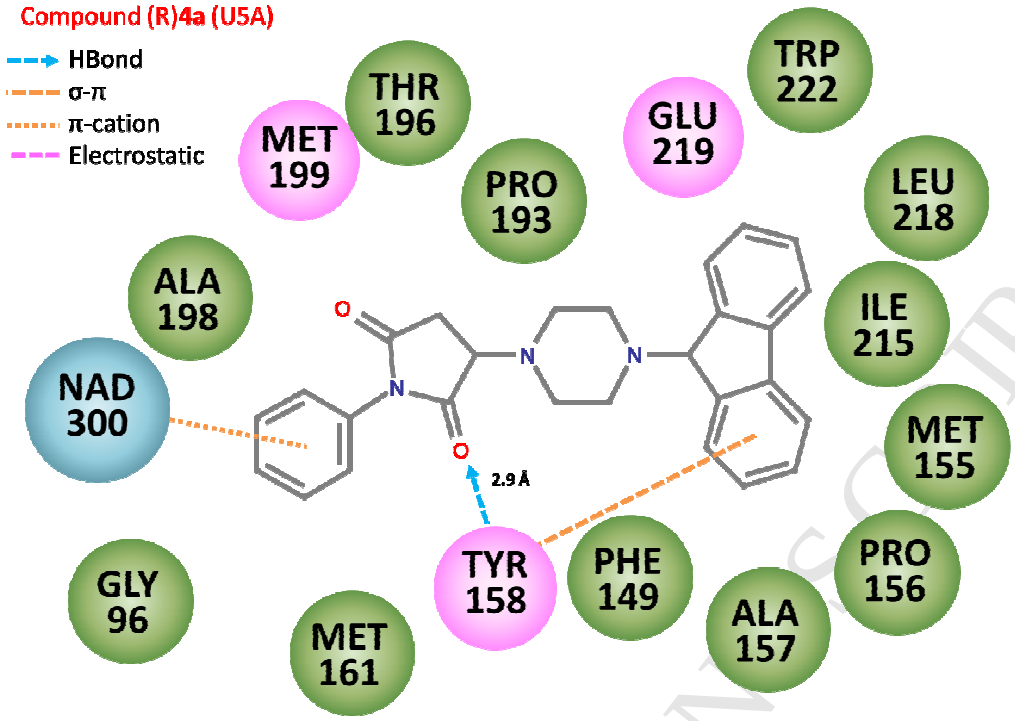

A - Compound **4a**, *S*-enantiomer (D5A) best pose.

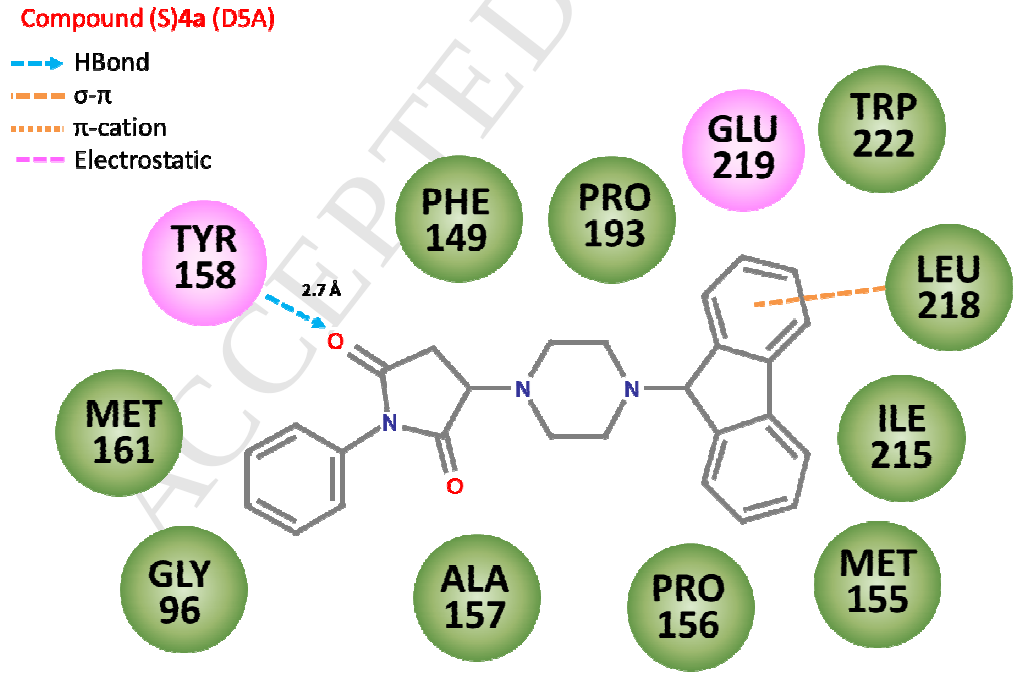

B - Compound **4a**, *R*-enantiomer (U5A) best pose.

SIFig.3 - 2D ligand-protein interaction diagrams after docking [*MOLEGRO_2006*] compound **4a** in structure 1P44a, 16 residues of active site (mainly upper NAD^+) were set flexible (GLY96, PHE97, MET103, GLY104, PHE149, PRO156, ALA157, TYR158, MET161, PRO193, ILE194, ALA198, ILE215, LEU218, GLU219, TRP222) and NAD^+ was used as cofactor.

Bibliographic information

[*MOLEGRO_2006*] R. Thomsen, M.H. Christensen (2006) MolDock: a new technique for high-accuracy molecular docking. *J. Med. Chem.* 49, 3315–3321.

[*DSV_2005*] Accelrys Software Inc., *Discovery Studio Modeling Environment, Release 3.0*, San Diego: Accelrys Software Inc. 2005-2010.

[*LASKOWSKI_2011*] R.A. Laskowski, M.B. Swindells (2011) LigPlot+: multiple ligand-protein interaction diagrams for drug discovery. *J. Chem. Inf. Model*. **51**, 2778-2786.